**TOPICAL REVIEW • OPEN ACCESS**

# Methods to improve antibacterial properties of PEEK: A review

To cite this article: Idil Uysal *et al* 2024 *Biomed. Mater.* **19** 022004





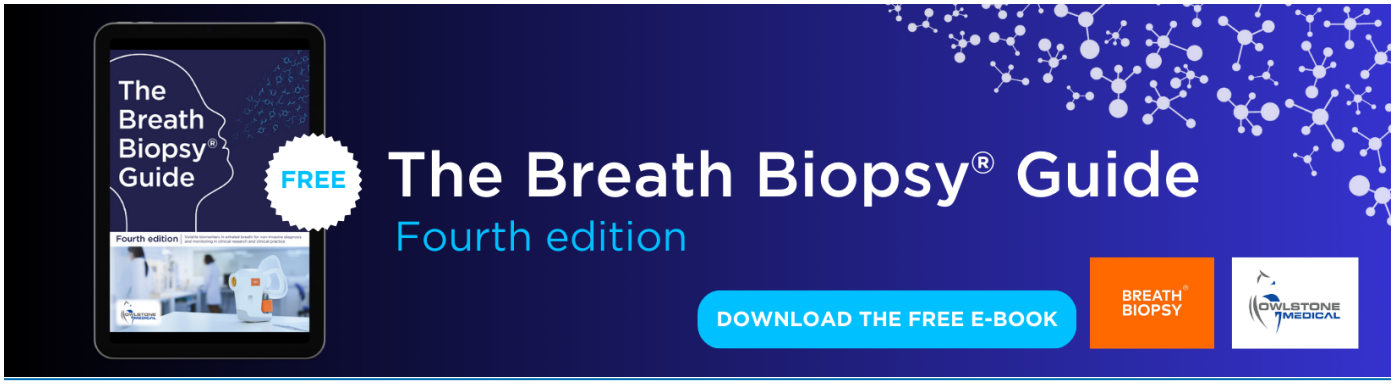

IOP Publishing Biomed. Mater. 19 (2024) 022004 https://doi.org/10.1088/1748-605X/ad2a3d

Biomedical Materials



TOPICAL REVIEW

# Methods to improve antibacterial properties of PEEK: A review

Idil Uysal[1,3], Ayşen Tezcaner[1,2,3] and Zafer Evis[1,2,3,*]

[1] Department of Biomedical Engineering, Middle East Technical University, 06800 Ankara, Turkey
[2] Department of Engineering Sciences, Middle East Technical University, 06800 Ankara, Turkey
[3] Present address: Middle East Technical University, Universiteler Mahallesi, Dumlupinar Blv. No:1, 06800 Cankaya Ankara, Turkey.
[*] Author to whom any correspondence should be addressed.

**E-mail:** evis@metu.edu.tr

**Keywords:** PEEK, antibacterial rate, biomedical applications, surface modifications

OPEN ACCESS

RECEIVED
24 July 2023

REVISED
15 January 2024

ACCEPTED FOR PUBLICATION
16 February 2024

PUBLISHED
29 February 2024



## Abstract

As a thermoplastic and bioinert polymer, polyether ether ketone (PEEK) serves as spine implants, femoral stems, cranial implants, and joint arthroplasty implants due to its mechanical properties resembling the cortical bone, chemical stability, and radiolucency. Although there are standards and antibiotic treatments for infection control during and after surgery, the infection risk is lowered but can not be eliminated. The antibacterial properties of PEEK implants should be improved to provide better infection control. This review includes the strategies for enhancing the antibacterial properties of PEEK in four categories: immobilization of functional materials and functional groups, forming nanocomposites, changing surface topography, and coating with antibacterial material. The measuring methods of antibacterial properties of the current studies of PEEK are explained in detail under quantitative, qualitative, and *in vivo* methods. The mechanisms of bacterial inhibition by reactive oxygen species generation, contact killing, trap killing, and limited bacterial adhesion on hydrophobic surfaces are explained with corresponding antibacterial compounds or techniques. The prospective analysis of the current studies is done, and dual systems combining osteogenic and antibacterial agents immobilized on the surface of PEEK are found the promising solution for a better implant design.

## 1. Introduction

Improvements in establishing the standards to control infections in the operating rooms and antibiotic treatment during the surgical procedure result in low infection rates. Despite all the precautions, infection is the second reason for the revision of the orthopedic implant for total knee arthroplasty [1]. Besides the peri-surgical infection control procedures, implants with antibacterial properties gained importance. Implant design with an antibacterial effect decreases the infection risk and accelerates the osteoblast adhesion to the surface, directly impacting the operation's success.

The factors affecting bacterial adhesion and biofilm formation are defined as surface roughness, surface charge, surface free energy, and hydrophobicity. Surface roughness should be above 0.2 μm to promote bacterial adhesion with a positive correlation. On the other hand, there is no correlation between bacterial adhesion and surface roughness below $R_a < 0.2$ μm [2]. Hydrophobicity is another factor that affects bacterial adhesion. As hydrophobicity increases, bacterial adhesion decreases [3]. Besides the surface properties, releasing materials with antibacterial effects enhances bacterial inhibition.

Polyether ether ketone (PEEK) is a semi-crystalline thermoplastic polymer that is used in industrial applications such as aircraft [4] and turbine blades [5, 6], missile connectors and radomes, cable insulation, acid pipelines, valve and pump parts, bearings [6], orthopedic and spine implants [7–9] and recently, fuel cell membranes when it is sulfonated [10, 11]. The distinctive properties that enable such applications can be listed as resistance to temperature, chemicals, radiation, and the environment [6]. Moreover, mechanical properties such as cut-through resistance, fatigue resistance, and abrasion resistance make PEEK a raw material candidate for challenging conditions [6].

PEEK polymer commercially emerged as a biomaterial for implants in 1998 [12]. As a high-performance polymer, it has become an alternative

for metal implant components in orthopedics [7] and trauma [13]. In terms of orthopedics, spine implants [8, 9], femoral stems, cranial implants [14, 15], and joint arthroplasty [16] are the products available on the market. The stability, biocompatibility, radiolucency, and mechanical properties similar to cortical bone make PEEK a good candidate for biomedical applications [17]. It can be formed easily in different shapes by using 3D printing techniques and can be customized [18]. Beacuse of its anti-wear performance, it is used in knee and hip joint replacements [18]. It is a radiolucent polymer; therefore, the defects can be observed easily by x-ray compared to metal implants [19].

Clinical studies that use PEEK as an implant material include the cervical area in cervical degenerative disc disease treatment, cranioplasty, and face reconstruction [20]. The comparison between pure PEEK cages and iliac crest autografts showed that PEEK cages serve as the substitutes for fusion with an effective restoration of physiological curvature and the intervertebral height and a facilitated radiological follow-up [21]. Another clinical application was cranioplasty. Compared to titanium implants, the failure rate decreased from 25% to 12.5% after using pure PEEK cranial implants, according to the retrospective records of patients [22]. Face reconstruction with pure PEEK was applied to four patients, and ease of working and high durability were the main advantages [23]. Another clinical case included 3D printed PEEK grafts for mandibular defects. It provided primary security and decreased the stress shielding effect compared to the metallic implants [24, 25]. In the field of dentistry, PEEK-based dentures, crowns, and bridges were produced by additive manufacturing [26]. Artificial teeth and double crown retained dental prostheses were implemented in the patients, and satisfactory results were reported in the clinical cases [26].

As a synthetic polymer, PEEK is suitable for extrusion/drawing-based techniques or additive manufacturing techniques based on powder bed fusion [24, 27]. 3D printing makes PEEK a good candidate for the complex geometries of bone implants. Moreover, the properties essential for bone implants can be tailored by processing parameters and functional additives. In terms of processing parameters of fused filament functioning of PEEK, nozzle temperature and layer height significantly affected surface roughness, elastic modulus, and ultimate tensile strength [28]. The printing techniques such as selective laser sintering and fused deposition modeling enabled the addition of functional materials such as graphene nanoparticles, carbon nanotubes, graphene oxide, titanium dioxide, aluminum dioxide, zirconium dioxide, or hydroxyapatite (HA) into the PEEK structure [24, 29]. The composite materials showed good mechanical properties such as tensile strength, compressive strength, and elastic modulus and increased osteogenic differentiation [24, 29]. Composites of PEEK and Hydroxyapatite (HA) with percentages of 20 and 40 were produced by fused filament fabrication for better osteogenic properties [30]. The composite increased the cell density and expressions of RunX2, OCN, ALP, and Collagen Type 1 genes as cell differentiation indicators. *In vivo* experiments showed that bone formation volume increased and the gap between the host bone and the scaffold decreased with HA addition [30].

Pure PEEK as a heart valve was simulated, showing high durability and smooth operation. Pure PEEK became an alternative biomaterial to produce pumps for intracardiac left and right ventricular assistance [20]. The equivalent modulus (0.5–17.3 MPa) and tensile strength (0.7–8.3 MPa) of PEEK costal cartilage produced with the 3D printing method gave similar results with natural costal cartilage (Elastic modulus: 8.7–12.6 MPa, tensile strength: 4–7 MPa) [31]. PEEK polymer has −OH groups at chain endings, resulting in a negative surface charge at pH 7 and an isoelectric point of about 4.5 [32].

Infection control is one factor that defines the success of the intervention. It dramatically impacts the revision, stability, or rejection of the implant by increasing the rates of morbidity, mortality, and medical costs [1]. Therefore, antibacterial properties are essential to prevent implant rejection. PEEK polymer biofilm formation showed an exponential increase for bacterial colonies such as *S. epidermidis, S. aureus, P. aeruginosa*, and *E. coli*. On the other hand, it showed a linear increase for *Enterococcus*. PEEK showed the highest biofilm affinity compared to Ti (up to 6.7 times higher) and $Si_3N_4$ surfaces (up to 16 times higher for as-fired samples). Similarly, the number of live bacteria is the highest, up to 30 fold for PEEK compared to $Si_3N_4$ as-fired surface [32]. The effects of production techniques on bacterial adhesion in dental applications were analyzed. Among commercial PEEK dental products, there were no significant differences between injected molded samples and printed samples of PEEK in adhesion of *S. sanguinis*. In contrast, pressed PEEK samples showed significantly higher adhesion [33]. On the other hand, another bacteria, *S. mutans*, had no differences in adhesion based on the manufacturing technique [33].

Since 1985, studies on PEEK polymer have shown an exponentially increasing trend. When the list of the records of search from Web of Science, Scopus, and PubMed indexes based on keywords 'PEEK', 'Polyether ether ketone', 'Poly-ether-ether-ketone', 'Polyetheretherketone', 'Poly ether ether ketone' is refined to those records related to antibacterial properties of PEEK by searching the keyword 'bacteria' and 'microbial' only 3 records are found for antibacterial properties of PEEK between years 1996 and 2009. The number of studies started to increase in

2010 and there were 16 articles published between 2010 and 2014. In the next five years (between 2015 and 2019), ∼4.1-fold increase in articles is seen. There are 169 papers published between the years 2020 and September 2023. It is obviously seen that as the share of PEEK as a raw material in the medical device industry grows, the studies related to its antibacterial properties will continue to increase.

The antibacterial properties of orthopedic implants are as essential as mechanical and osteogenic properties. PEEK usage has a high potential in orthopedic implants. The review articles published in the last four years (between 2020 and September 2023) included most of the modification methods, especially surface modifications, with detailed techniques grouped into physical, chemical, and biological modifications [34–39]. A few reviews included composite production as a method to increase the antibacterial properties of PEEK [34, 39]. Moreover, most of the reviews presented the antibacterial properties under the topic of the improvements of osseointegration [18, 38]. In terms of clinical perspectives, the antibacterial properties of PEEK have been mostly studied in the scope of dental applications since the biofilm formation has been the main problem for implant integration [34, 37, 38, 40–42]. The development of PEEK in bone tissue engineering for orthopedic surgery has also been covered in terms of clinical perspectives [43]. This review presents a comprehensive up-to-date overview of the studies focused mainly on the improvements of the antibacterial properties of PEEK for biomedical applications. The improvements were discussed in terms of immobilization of antibacterial materials on the PEEK surface, coating antibacterial material on PEEK, production of composites, and changing the surface texture to obtain an antibacterial property. Testing methods and promising results are summarized to support the future studies in the field to carry the improvements to one step further. This review is distinctive in presenting a broad perspective of measurement methods for testing the antibacterial properties of PEEK, and mechanisms of bacterial inhibition achieved after modification of PEEK are discussed in depth. It covers all modification methods specific to antibacterial properties without limiting the application area in the biomedical field. The design requirements for the best antibacterial properties are discussed as a future perspective.

## 2. Measuring strategies of antibacterial activity of PEEK

There are different strategies to observe the antibacterial property of PEEK. Qualitative methods with different imaging techniques, quantitative methods, and *in vivo* studies are applied. Table 1 summarizes the definitions of the methods applied to measure the antibacterial properties of PEEK. Although the quantitative methods are found adequate to discover the antibacterial rate of a sample in most of the studies, the support of qualitative methods should be considered. For the studies in which quantitative analysis is applied in the short term, observing the bacterial cell morphology gives the researcher insight into the later stages of bacterial growth. Therefore, it would be better to support quantitative analysis with a qualitative one for short-term analysis to obtain valuable information about the time frame, which enables making comments about the race-for-the-surface concept. In this context, antibacterial longevity and kinetic tests deserve considerable attention due to the importance of timing among those methods. After the implantation, osteoblasts and bacteria compete for the attachment on the surface. If the antibacterial property lasts an adequate time for the osteoblast attachment, implant rejection is prevented. *S. aureus* is the most tested bacteria type to observe antibacterial properties. It has been a good choice since *S. aureus* and *S. epidermidis* form 66% of the pathogenic species among orthopedic clinical isolates of implant-related infections [1]. However, the antibacterial effect with a broad spectrum should be targeted to obtain an effective biomaterial. In terms of measuring methods, colony-forming unit calculation and calorimetric assays have given accurate and quantitative results. Moreover, measuring antibacterial longevity provides information about the loading amount of the antibacterial agent for release to support osteoblasts for race for the surface.

The most common methods used are plate counting and measuring zone of inhibition due to their ease of application. The plate counting method enables researchers to discriminate between dead or live bacteria and adherent or planktonic bacteria. Therefore, a more detailed analysis is obtained in colony forming unit (CFU)/ml, a parameter used in the medical device industry to calculate the bioburden. Therefore, making comparisons for the real cases is possible. Intracellular reactive oxygen species (ROS) and glutathione depletion assays are specific to antibacterial mechanisms, and their application area is limited. Phagocytic activation of macrophages is another technique to measure the antibacterial efficiency of the PEEK samples. It is helpful regarding the body's reaction to the bacteria and is like an *in vivo* simulation. Pathogenic gene detection is another method that gives more specific detection of the pathogens and gives more accurate results in terms of the implant's safety compared to colorimetric assays and plate counting methods.

*In vivo* studies provide valuable information related to the rate of inflammation after implant replacement; they are essential to comment on the success of the implant. However, due to ethical considerations, high costs, and time limitations, *in vivo*

**Table 1.** Measurement methods of antibacterial property of PEEK.

| Type | Name of the method | Description of the method | Reference |
|---|---|---|---|
| Quantitative | Plate counting method | The samples are incubated in a bacterial suspension, and the rinse medium, including bacteria, is added to an agar plate. The number of colonies formed on the agar plate is counted after incubation of a specified time.<br>- Colony forming unit (CFU)/ml is used to quantify the number of bacteria.<br>- Some studies use bacterial viability kits with fluorescent dyes to discriminate live bacteria (SYTO 9) and dead bacteria (PI) by image analysis.<br>- Some studies separate bacteria into free-swimming (planktonic) and biofilm (adherent) modes. The adherent bacteria are separated from the samples by sonication and vortex.<br>- The antibacterial rate is calculated by the formula below;<br>Antibacterial rate (%) = $(OD_{PEEK} - OD_{\text{modified PEEK sample}})/OD_{PEEK} \times 100\%$, where OD is the optical density. | [32, 44–50] |
| | Measuring zone of inhibition (Kirby Bauer Test) | Each sample's zone of inhibition in mm is measured after the samples are incubated with bacterial inoculums with semi-confluent growth for a specified time. | [48, 51] |
| | Bacterial attachment | The sterile samples are co-cultured with a specified amount of bacterial suspension for a specified time interval. After removing the non-adherent bacteria, ultrasonication is applied to detach the adherent bacteria. The bacterial colonies are counted after spreading on the agar plate. | [3] |
| | Membrane permeability | The medium is refreshed with and an addition of sodium dodecyl sulfate (SDS) (0.1% concentration) after incubation of samples with bacterial cells for a specified time. Optical density was measured at 570 nm. Lower optical density showed a strong ability to rupture the bacterial membrane and higher antibacterial properties. | [52] |
| | Colorimetric assay | The assay is based on staining the attached cells to the sample after culturing with a specified concentration of bacteria. Crystal violet, formazan dyes, and Alamar Blue reagent were used in studies of PEEK. | [44, 53, 54] |
| | Antibacterial kinetic test | The absorbance of bacterial suspensions at 600 nm is recorded after incubating the samples with a specified number of bacterial solutions at defined time intervals. | [55] |
| | Phagocytic activity evaluation of macrophages | Macrophage cells are cultured with the bacterial solution, including fluorescently dyed bacterial cells. Bacterium-infected cells are plated in a different well plate after flow cytometry. Extracellular bacteria are killed by incubation with gentamicin. The intracellular bacteria are released by using 1% Triton. The spread plate method counts all collected bacteria. | [56] |

(Continued.)

**Table 1.** (Continued.)

| | | | |
|---|---|---|---|
| | Intracellular ROS assay: | The fluorescence intensity of 2′,7′<br>- dichlorodihydrofluorescein diacetate is measured after one day of incubation by ROS assay kit. | [56] |
| | Glutathione depletion assay | The detection of glutathione depletion in the infectious environment indicates oxidative stress. Ellman's assay is used to detect the capability of glutathione breakage. The loss of glutathione percentage is calculated by the formula below with the absorbances collected at 420. Loss of Glutathione (%) $= (A_{\text{negative control}} - A_{\text{sample}})/A_{\text{negative control}} \times 100\%$<br>A: absorbance of the corresponding samples. | [57] |
| | Antibacterial longevity | The incubation period extends up to 28 d. The samples are collected at a specified time point. Colony formation unit calculation is applied after one day of incubation. | [58] |
| | Pathogenic gene detection by real-time polymerase chain reaction (PCR) | Real-time PCR was applied to detect pathogenic gene expression. *m*RNA levels of the *Fim* gene for *P. gingivalis* and the *Gtf* gene for *S. mutans* were analyzed as pathogenic genes. | [59] |
| Qualitative | Biofilm formation and bacterial attachment observed by SEM (Scanning Electron Microscopy) | The bacteria are seeded on the samples at a specific density. The samples are incubated in tryptic soy broth for a specified time. The bacterial cells are fixed using 2.5% glutaraldehyde in 0.1 M sodium cacodylate and 0.1 M sucrose buffer for 30 min. The samples are dehydrated with ethanol (concentrations from 30% to 100%). Critical point drying in $CO_2$ is applied before sputter coating with Au/Pt. The biofilm formation and the adhesion of bacteria are observed by SEM. | [48, 60] |
| | Bacterium infected macrophages observed by fluorescence microscope | Macrophage cells, including fluorescently dyed bacterial cells, are cultured with the bacterial solution. Bacterium-infected cells are plated in a different well plate after flow cytometry. A fluorescence microscope generates the images after staining the cytoskeleton by phalloidin. | [56] |
| *In vivo* experiments | | - MRI and Micro CT were used to observe the tissue around the implant with a specified bacterial concentration.<br>- Staining with hematoxylin, eosin, or Giemsa investigates inflammatory tissue proliferation and colony distribution.<br>- Periosteum reaction against bacterial infection or osteomyelitis model system is preferred to observe the infection.<br>- Tibia and femoral condyle have been the regions studied before | [50, 58, 61, 62] |

studies have been applied in studies less than quantitative and qualitative methods.

## 3. The mechanisms of the antibacterial effect of modified PEEK

There are mechanisms proposed for the antibacterial ability of the modification techniques. These are ROS generation, contact reactions between the bacterial cell membrane and the antibacterial agent, the hydrophobicity of the surface, trap killing, and the nanoblade effect (figure 1). Among those mechanisms, ROS generation and contact-killing mechanisms have been widely observed in the studies. On the other hand, relatively few studies have studied the mechanism of surface hydrophobicity or trap killing and

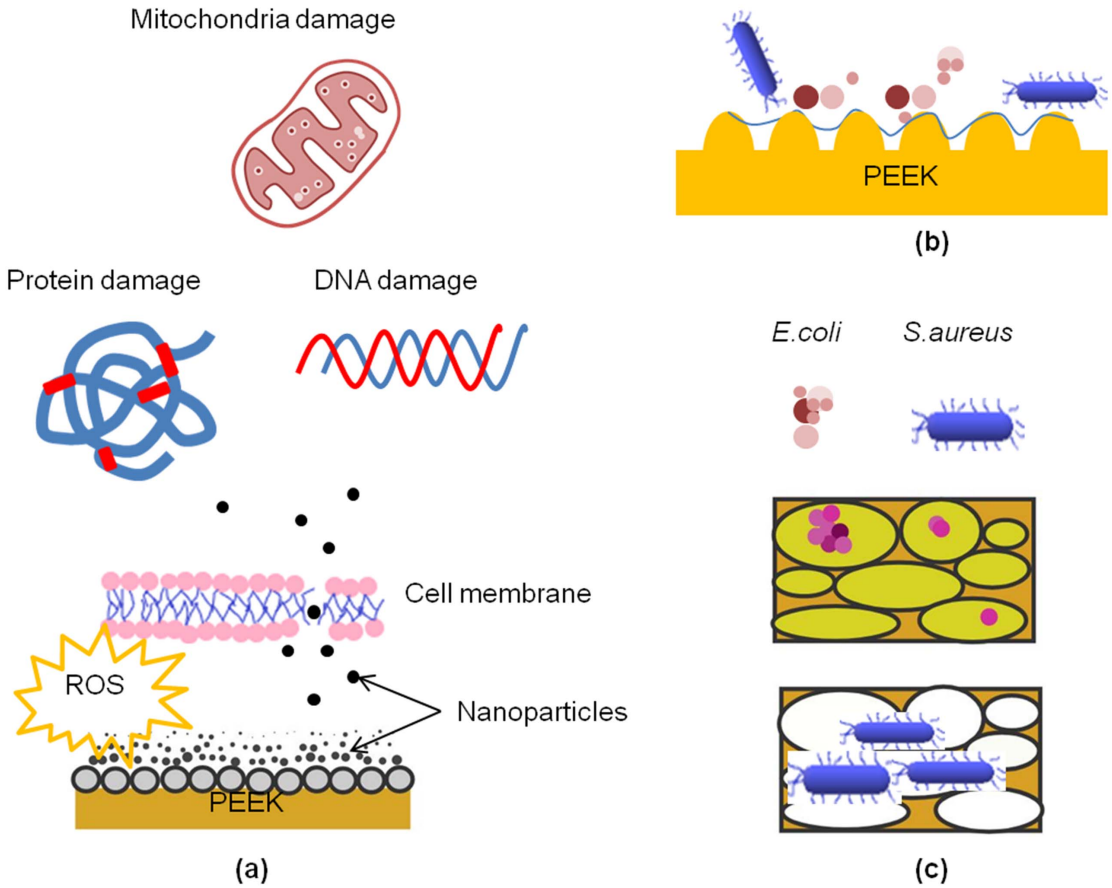


**Figure 1.** The mechanisms of the antibacterial effect of modified PEEK: (a) ROS generation and contact killing: Electrostatic interactions between bacterial cell membrane and antibacterial ions deteriorate the integrity of bacterial cell membrane. The antibacterial nanoparticles pass through the cell membrane and trigger ROS generation, which results in protein damage, DNA damage, or mitochondria damage [52, 62–65]. Adapted with permission from [66]. Copyright (2017) American Chemical Society. (b) Hydrophobicity of the surface: prevents hydrophilic bacteria from attaching the surface. Either coating can provide hydrophobicity with a hydrophobic material or change the surface texture [48, 67]. (c) Trap killing: Bacteria are trapped and can not form a biofilm on the porous surface of the material. The size of pores and bacteria determines the efficiency of the method [62, 68].

nano-blade effect. In each method, an optimization is required. The amount of the metal ion, compound, or drug should be adjusted to find a perfect composition for the bacterial detachment concurrently with cell attachment since all antibacterial mechanisms (contact killing, generation of ROS, and increase the hydrophobicity of the surface mechanisms) also have similar effects on cells. In this sense, the modification should serve the race-for-the-surface concept, and the duration of the effectiveness of the modification should be adjusted. For the nano-blade effect or trap killing, the dimensions of the topographical changes should be optimized. Controlling the dimensions on the surface topography at the micron level is more complex than controlling the composition of the modification. Therefore, the modifications for contact killing and ROS generation are widely studied compared to modifications for nano-blade effect or trap killing.

### 3.1. Reactive oxygen species (ROS) generation and contact killing

ROS, one of the 'reactive species' with molecular oxygen, has gained importance in biology and medicine. They are formed by reduction-oxidation reactions and by electronic excitation. They are separated into non-radical and free-radical ROS [69]. Non-radical species include hydrogen peroxide ($H_2O_2$), organic hydroperoxides (ROOH), singlet molecular oxygen ($^1O_2$), electronically excited carbonyl (R–C = O), ozone ($O_3$), hypochlorous acid (HOCl) and hypobromous acid (HOBr) [69]. The examples of the free radical ROS are superoxide anion radical ($O_2\cdot^-$), hydroxyl radical (·OH), peroxyl radical (ROO·), and alkoxyl radical (RO·) [69]. ROS causes oxidative distress, which is a term used for molecular damage. Metal ions, drugs, and ionizing radiation are counted as exogenous sources of ROS [69–73]. ROS have considerable roles in homeostasis and cell signaling.

However, if the balance deteriorates, it causes irreversible DNA damage. In the other mechanism, contact killing, electrostatic interaction destroys cell membrane integrity. Most of the metal ions with positive charges deterioriate the negatively charged cell membrane and result in increase in permeability of rupture of the membrane. Those ions pass through the cell membrane and trigger the oxidative distress by creating ROS.

PEEK powder and nano-ZnO were melt blended to obtain a composite for a filler material of artificial joint. The composite showed an antibacterial effect on *E. coli* (42%) and *S. aureus* (39%) when added at 7.5 wt. % [63]. The mechanism was explained by two methods: contact reaction and photocatalytic reaction. In contact reaction mechanism, electrostatic interaction occurs between the positively charged Zinc ions and the negatively charged bacterial membrane [63]. Another mechanism targets the proteases. After adding 7.5 wt. % to the PEEK composite, the zinc ion inactivates the protease, an enzyme that breaks down the protein into peptides, and the physiological activity of bacterial cells deteriorates [63]. The same antibacterial mechanism was explained for PEEK implants coated with dexamethasone-loaded Zn and Mg-containing organic frameworks for bone graft applications [74]. Likewise, in a composite system, the zinc ions become integrated into the bacterial membrane by binding hydrophobic imidazole amino and carboxyl groups and destroy the cell membrane, which results in the leakage of the cell content in the coating system [63, 74]. According to the results, an inhibition rate of 100% against *S. aureus* and *E. coli* was obtained for the samples coated with Zn-Mg-metal organic frameworks [74].

Photocatalytic activity includes the activation of ROS with the interaction between ZnO and UV irradiation. The strong chemical activity generated by ROS kills the bacteria [63].

Another material for both contact reaction and ROS generation mechanisms proposed was Ag nanoparticles [64]. When Ag nanoparticles were decorated onto PEEK/Gelatin blend hydrogel, the antibacterial rates increased from 57.1% to 88.4% against *S. aureus*. Similarly, the antibacterial rate reached 95.7% from 61.8% against *E. coli* [64].

There are dual or ternary systems that combine antibiotics and ceramics or nanoparticles to enhance antibacterial properties or obtain antibacterial and osteogenic properties simultaneously for biomedical applications [75, 76]. For example, in a gentamicin-loaded brushite system, only gentamicin possessed antibacterial properties [75]. On the other hand, a synergistic effect formed when Ag nanoparticles and gentamicin sulfate (GS) were coated together on sulfonated PEEK [52]. Two mechanisms were proposed to explain the antibacterial property. The first one is the binding ability of these molecules to biological elements like DNA, protein, or cofactors due to their high affinity for amines, phosphates, and thiol groups and disturbing cell metabolism. GS binds to the 30S subunit of the ribosome and deteriorates protein synthesis. The synergistic effect of localized GS and Ag nanoparticles causes an increase in ROS production. They scavenge the intracellular reductase enzymes, and the catalytic process of ROS production is boosted. Ag nanoparticles and GS stimulate nicotinamide adenine dinucleotide oxidation. Hyperactivation of the electron transport chain leads to superoxide formation. ROS formation by the Fenton reaction is triggered by the ferrous irons formed after the damage of iron-sulfur clusters by superoxide formation [52]. Direct interaction of Ag nanoparticles with bacteria results in cytoplasm leakage and bacteriolysis [77].

$Cu^{2+}$ ion immobilization on PEEK with polydopamine (PDA) or magnetron sputtering was used to obtain antibacterial implants for biomedical applications [62, 65]. In a study, magnetron sputtering was used for immobilization, and sessile *Methicillin resistant S.aureus (MRSA)* bacteria amount decreased from $84.77 \times 10^5$ CFU (PEEK) to $4.93 \times 10^5$ CFU (PEEK with immobilized $Cu^{2+}$ (49 μg/L)) [62]. $Cu^{2+}$ was also used for ROS generation and contact-killing mechanisms against *MRSA*. The contact-killing occurred with the destruction of the cell membrane by $Cu^{2+}$ ions by their electrostatic interaction with the bacterial membrane. $Cu^{2+}$ ions in the bacterial cell cause the generation of ROS by Fenton reactions, inhibition of RNA/DNA replication due to toxicity, protein denaturation, and DNA cleavage after binding proteins and DNA [62, 65].

It was reported that Au nanoparticles coated on carbon fiber reinforced PEEK composites by metal-organic chemical vapor deposition and physical vapor deposition techniques to obtain a functionalized implant surface resulted in inhibition against *S. aureus, S. epidemidis, Str. pyogenes, P. aeruginosa, Ent. faecium* [78]. Bacterial colonies grew larger than 700 for carbon fiber-reinforced PEEK, whereas the value decreased to 300–500 colonies after coating with Au [78]. Like in $Cu^{2+}$ and $Ag^{+}$, the mechanisms for Au were explained by the destruction of cell membrane and ROS production after the change in the membrane charge by interaction of Au nanoparticles with the phospholipids in the bacterial cell wall [78]. Another nanomaterial that causes bacterial inhibition with the same two mechanisms was *n*-$TiO_2$. The antibacterial effect of *n*-$TiO_2$ was explained by creating mechanical stress and generating ROS. PEEK and polyglycolic acid blend with *n*-$TiO_2$ powders to obtain a scaffold for bone tissue engineering applications. By adding 5 wt. % of *n*-$TiO_2$, an antibacterial rate, higher than 85% was obtained against *S. aureus* and *E. coli* [79]. The mechanical stress

generated by the contact action deformed the bacterial cell membrane. Moreover, ROS production was triggered by the reaction between water, oxygen, and $n$-$TiO_2$. ROS production resulted in oxidative stress that collapsed the bacterial antioxidant defense system [79].

Three mechanisms for their effect were proposed for antibiotics (vancomycin, gentamicin, ampicillin, amoxicillin, etc.). These are an increase in cell membrane permeability followed by loss of its function, prevention of replication, and inhibition of cell wall synthesis [80, 81]. Resveratrol, an antioxidant, has been used for its antibacterial properties. The mechanism proposed was similar to antibiotics and defined as the increase in cell permeability and inhibition of cell wall synthesis [82].

A single mechanism based on electrostatic interactions to penetrate the bacterial cell wall was proposed for chitosan and peptide-based compounds to explain the antibacterial effect. A solution including chitosan, hydroxyapatite (HA), and PEEK solution was applied on stainless steel (316L) by electrophoretic deposition to obtain a composite coating for biomedical applications [83]. Chitosan increased the bacteriostatic percentage to above 80% against *S. aureus* and *E. coli* [83]. When chitosan was coated directly onto PEEK by UV-induced graft polymerization and wet chemical methods, the number of *E. coli* was reduced by about 70%. In those systems, $NH^{3+}$ groups in the structure of chitosan form osmotic imbalances when chitosan was in contact with the negatively charged bacterial cell wall. When cationic groups such as $NH_2$ interact with the negative bacterial cell surface, surface zeta potential difference is induced, causing damage to the bacterial cell membrane [84]. Another mechanism related to the electrostatic interactions is the deformation of peptidoglycans in the cell wall. Such damage causes an increase in the penetration/permeability of vital intracellular molecules such as potassium, proteins with low molecular weight, and their eventual loss [83].

On the other hand, the mechanism of the antibacterial effect of the K-12 protein is related to its amino acid sequence. In its sequence, five positively charged amine groups attract negatively charged bacterial cells and disrupt bacterial cell wall via the charge effect [85–87]. Antibacterial peptide GL13K uses the same mechanism against *S. aureus* [88].

Other choices that can be used for cell wall destruction of bacteria are lactam and lysozyme. Lysozyme is a protein that can break the $\beta$-1,4-glycosidic bond between *N*-acetylcytidylic acid and *N*-acetylglucosaminoglucose to convert insoluble mucopolysaccharide into soluble glycopeptides in bacteria. Then, the destruction of the cell wall occurs [89]. PEEK surface coated with PDA-modified nanohydroxyapatite and lysozyme to obtain orthopedic implants with a functionalized surface. The antibacterial ratio of 98.7% and 96.1% against *S. aureus* and *E. coli* were obtained with the aforementioned mechanism [89].

On the other hand, the bromine and chlorine content of the lactam inhibits the biofilm of *S. mutans* [90]. Lactam was used as a coating constituent combined with PEEK and dip-coated on a glass-based substrate to obtain an oral implantology biomaterial resistant to biofilm formation. The absorbance of spectrophotometry at 630 nm for biofilm formation was decreased from 0.09 to 0.01 when lactam was added to the coating [90].

Different mechanisms were proposed for the considerable antibacterial effect of PEEK and nanofluorohydroxyapatite composites [91]. The antibacterial effect of fluoride was explained by the inhibition of the glycolytic enzyme enolase, the proton-extruding ATPase, and bacterial colonization and competition. Moreover, some enzymes such as acid phosphatase, pyrophosphatase, peroxidase, and catalase were affected by fluoride ions, and the disintegration of bacteria occurs. Another factor was the positive effect of nanofluorohydroxyapatite on cell adhesion. If the cell adhesion on the implant's surface is higher than bacterial adhesion, bacterial colonization is prevented [91].

Black phosphorus inhibited *S. aureus* by only the generation of ROS [92]. Similarly, the bacterial reduction with $ZrO_2$ nanoparticles on the surface stemmed from the formation of ROS. An alkaline effect by forming hydroxyl groups around $ZrO_2$ increased local pH [93]. The change in the pH of the environment affected the bacteria. For example, bioglass 45S5 particles in the PEEK matrix increased the pH to a level that bacteria could not live [67]. Adding GO into PEEK with 0.02 wt. % increased the antibacterial ratio from 82.10% to 99.56% against *S. aureus*, which has a single cell wall. The antibacterial mechanism of GO was explained by ROS generation and the nanoblade effect. GO induced the generation of hydroxyl radicals, singlet molecular oxygen, and superoxide anions which damaged DNA, proteins, and intracellular components in terms of ROS generation [94].

### 3.2. Hydrophobicity of the surface

Bacteria are more likely to attach to hydrophilic surfaces. However, this property changes according to the bacteria type with different surface tensions [95, 96]. The hydrophobic surface is counted as one reason for the antibacterial property. PEEK is a hydrophobic polymer. Coating with more hydrophobic materials increases the water contact angle of PEEK. Ion doping can alter hydrophobicity. For example, although the Ag ion is hydrophilic, it increased the water contact angle of PEEK coated with $TiO_2$/ poly dimethylsiloxane (PDMS) hybrid structure depending on the amount of doping [48]. As the Ag content in the structure was increased, the surface roughness was altered, which improved hydrophobicity. Similarly,

coatings formed by the addition of bioglass 45S5 particles into the PEEK matrix showed antibacterial properties against *E. coli* due to the formation of needle-like structures on the surface that increased hydrophobicity [67].

### 3.3. Trap killing and nano-blade effect

Trap killing and nano-blade effects are related to the physical interaction between bacteria and material surface. For example, trap killing was observed when the bacteria (pore size: ∼0.5 μm) were trapped in the porous surface (pore size: ∼1 μm) of $Cu^{2+}$ ion immobilized surfaces, and proliferation was restricted [62]. ZnO/GO coatings on PEEK have shown trap killing mechanism against *F. nucleatum*. GO layers trapped the bacteria and prevented biofilm formation [68]. Another mechanism proposed for GO was the nano-blade effect which was explained by bacterial membrane destruction after contact with the sharp edges of GO nanosheets [94].

## 4. The methods to improve the antibacterial properties of PEEK

As mentioned in the introduction, improving the antibacterial properties of PEEK affects the success of orthopedic operations. The methods to improve the antibacterial properties of PEEK were analyzed and discussed under four different categories based on the production methods: (1) immobilization of functional materials and functional groups, (2) coating with antibacterial material, (3) forming composites and nanocomposites, (4) changing the surface topography.

### 4.1. Immobilization of functional materials and functional groups

The most widely used method to improve the antibacterial properties of PEEK is the immobilization of functional materials and functional groups on the surface of the material. The compounds immobilized onto the surface consist of antibacterial drugs (ampicillin and vancomycin), ions ($Zn^{2+}$, $Ag^{+}$, $Cu^{2+}$, F), peptides, functional groups such as $SO_3H$, NO, $–NH_2$, oxides (GO, $ZrO_2$).

The most common method for immobilization is dripping the solution of the antibacterial agent onto the functionalized or neat PEEK surface (figure 2). The dripping method is preferred to obtain more precise control over the material. It is an easy method, and a small amount of material can be used to observe the antibacterial properties. Similar methods, such as immersion and soaking, provide more surface area for the interaction of bacteria and antibacterial agents. Wet chemical methods are applied by immersion to immobilize functional materials onto PEEK [45]. For example, the carboxyl groups grafted PEEK was immersed in 0.1 wt.% EDC (1-(3-dimethylaminopropyl) −3-ethylcarbondiimide hydrochloride) solution and the pH of the solution were adjusted to 4.7 with acetic acid before the immersion into the solution with chitosan dissolved in acetic acid [45]. Immersion and soaking are easy to apply; however, they require given volume of the solution that the substrate can sink in. Table 2 summarizes the immobilization techniques of antibacterial materials onto a PEEK substrate. Since PEEK is a chemically inert material, the study uses PDA to immobilize the functional compounds. First, PEEK samples were coated with PDA as an adhesive layer. Then, the molecule with an antibacterial effect was added [47, 65, 74, 97, 98]. Some studies first produced a composite of functional material and PDA, and then coating was applied [61]. Sulfonation is another technique used to attach molecules onto chemically inert PEEK. It is the first modification applied in plenty of studies. After the sulfonation, $SO_3H$ ions were attached to the surface of PEEK, which had an inhibitory effect on *S.aureus* and *E.coli*. Depending on the process parameters and the amount of sulfur attached, the antibacterial rate changed [50, 99].

The concentration of the immobilized compound is important to provide antibacterial longevity. For example, 10 μg $ml^{-1}$ recombinant mouse beta-defensin-14 onto PEEK showed 80%–100% antibacterial effect against *E. coli* and *P. aeruginosa* after 28 d of incubation [58]. When smaller concentrations, such as 2 μg $ml^{-1}$, were applied, *P. aeruginosa* showed only 37.02% inhibition [58].

According to table 2, $Ag^{+}$ is a powerful antibacterial agent, and it was shown to increase antibacterial rates in 90% of all studies. Therefore, it is a widely used ion to add antibacterial properties to the biomaterials. However, the amount of the ion should be adjusted to provide biocompatibility. The antibacterial properties of the same compound can be adjusted by combining PDA and applying phototherapy. For example, GO had a moderate antibacterial rate if coated on a PEEK substrate $O_2$ and $OH^{-}$, generating much ROS [109].

In some studies, there were differences in responses of different types of bacteria. Most of the studies tested both Gram-negative and Gram-positive bacteria. In a study, GO showed moderate antibacterial properties on hydrophobic *E. coli*, but it did not affect hydrophilic*S. aureus* [106]. $ZrO_2$ was another compound that gave different results for different types of bacteria. A moderate effect was detected for *S. aureus*, whereas no antibacterial effect was seen for *E. coli* due to its stronger resistance to $ZrO_2$ nanoparticles. *E. coli* is a Gram-negative bacteria with an effective barrier (a complex cell membrane including lipopolysaccharide molecules) [93]. When the antibacterial compound was quaternary ammonium salt, the length of the alkyl chain of quaternary ammonium salt caused more effective inhibition of *S. aureus* than *E. coli* since *S. aureus*

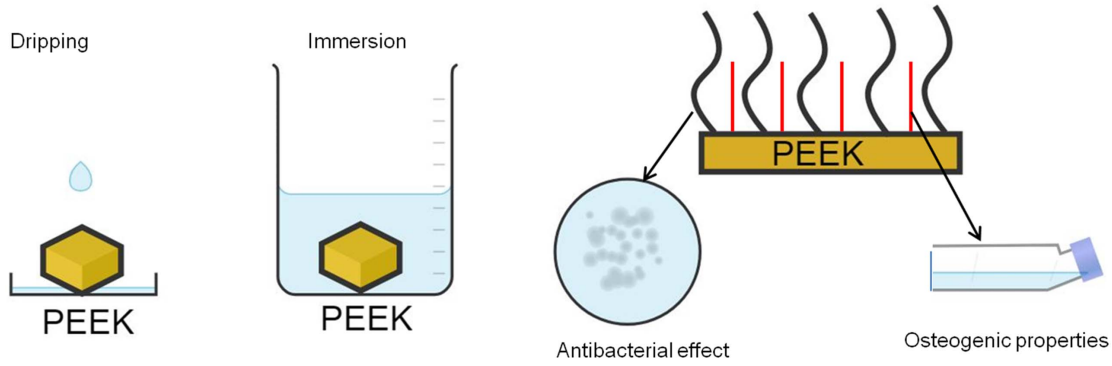


**Figure 2.** Immobilization of functional groups onto PEEK with the two most common methods, dripping and immersion. Antibacterial effect and osteogenic properties obtained by immobilization of two different materials offer solutions for a better implant design [50, 61].

was a Gram-positive bacteria [103]. Vancomycin was more effective on *S. aureus* than *E. coli* [76].

The difference between the antibacterial rate of planktonic and adherent bacteria may be observed in some studies. A sulfonation process followed by the immobilization of Cu nanoparticles on the PEEK surface gave a higher antibacterial rate on adherent *MRSA* than planktonic ones. It was explained by the synergistic effect of trap-killing and contact-killing mechanisms. Since adherent bacteria were trapped, they had more direct contact with the surface and they were more affected by Cu nanoparticles [62].

Besides antibacterial properties, osteogenic properties of the materials after the immobilization of molecules were widely studied. For example, osthole nanoparticles and berberine immobilized on sulfonated PEEK promoted osteogenesis [61]. Another dual-functional PEEK-based biomaterial was produced by mussle-inspired PDA. The coating containing osteogenic growth peptide and moxifloxacin hydrochloride loaded on sulfonated PEEK and sustained release was provided to prevent biofilm formation [50]. Similarly, dexamethasone and minocycline-loaded liposomes attached to a mussle-inspired PDA coating provided a dual effect, improved osseointegration, and antibacterial properties [47]. Besides antibacterial properties, the effects of the molecules below on osteogenic properties were studied: dexamethasone-loaded dual-metal–organic frameworks on PEEK promoted angiogenesis [74]. Recombinant mouse beta-defensin-14 [58], Ag-loaded PDA [97], Zn-loaded acrylic acid [105], Ag-immobilized hydroxyapatite [110], hinokitiol [102], GO [106], ethylenediamine [84], carboxymethyl chitosan and bone forming peptide [101], $Mn^{2+}$ and $Cu^{2+}$ immobilized on PDA [65], grafted modified poly ethylene glycol [104], resveratrol [82], GO nanosheets-PDA nanofilm-oligopeptite system [109], genistein [100], antimicrobial peptide KR-12 loaded on PDA [85].

*4.1.1. Methods of immobilization of functional groups and changing surface texture concurrently*

The cold plasma method changed the surface textures by increasing the surface roughness and adding nitrogen-containing groups to the structure [60]. Nitrogen-containing groups increased the positive charges on the PEEK surface, whereas the bacterial membrane was negatively charged. Therefore, it was expected to increase bacterial cell attachment on the PEEK surface due to electrostatic interactions. However, since the surface texture was changed and bacterial attachment mechanisms were dependent on many factors, such as topography, chemical composition, and hydrophilicity, an increase (∼26%) in the antibacterial efficiency after the cold plasma treatment with $N_2$ was observed [60]. The inhibition of bacterial growth in the presence of nitrogen-containing groups was the reason for the increase in the antibacterial rate [60, 111, 112].

Plasma immersion ion implantation is another technique to change the surface texture and composition of PEEK. In a study in which $ZrO_2$ ions were implemented by plasma immersion ion implantation, the antibacterial reduction of *S. aureus* was detected as 62.7% [93]. ROS formation explained the reduction due to $ZrO_2$ nanoparticles on the surface and the alkaline effect that was explained by the formation of hydroxyl groups around $ZrO_2$ and increased local pH [93].

Sulfonation is a standard method to obtain a porous structure on PEEK. Besides, this method attaches $SO_3H$ groups to the surface. $SO_3H$ groups decreased the bacterial viability on the surface depending on the sulfur content [50]. A composite of nano magnesium silicate and PEEK showed no antibacterial property against *E. coli* and *S. aureus*. On the other hand, the antibacterial rate increased to 98.29% and 99.76%, respectively, in 24 h after sulfonation [113].

**Table 2.** The antibacterial effect of the modification via immobilization of functional materials.

| | Modification method | Substrate | Material | High (Bacterial effect > 80%) | Moderate (Bacterial effect between 80%–50%) | Low (Bacterial effect < 50%) | Reference |
|---|---|---|---|---|---|---|---|
| Drugs, Peptides, Proteins and Polymers | Dripping and immersion | PDA-protected osthole nanoparticles loaded PEEK | Silk-fibroin and berberine | *S. aureus, S. epidermidis* | | | [61] |
| | Immersion | Mussle inspired PDA coated sulfonated PEEK | Moxifloxacin hydrochloride (1 mg $ml^{-1}$) and osteogenic growth peptide (100 μg $ml^{-1}$) | *S. aureus, E. coli* | | | [50] |
| | Immersion | Mussle inspired PDA coated sulfonated PEEK | Dexamethasone and minocycline loaded liposomes | *S. mutans* | | | [47] |
| | Dripping | Zn-Mg-organic framework coated on mussle inspired PDA coated PEEK | Dexamethasone | *S. aureus, E. coli* | | | [74] |
| | Dripping | Sulfonated and lyophilized PEEK | Recombinant mouse beta-defensin-14 | *S. aureus, P. aeruginosa* | | | [58] |
| | Dipping | Sulfonated Ta (40 vol %)/PEEK composite | Genistein (1000 μg $ml^{-1}$) | *S. aureus, E. coli* | | | [100] |
| | Immersion | PEEK/magnesium calcium silicate | Resveratrol | *S. aureus, E. coli* | | | [82] |
| | Covalent grafting | Carbon fiber reinforced PEEK/nano hydroxyapatite composite | CMC[b] | | | *S. aureus* | [101] |
| | Dripping | Nano bioglass (30 wt.%)/PEEK composite | Hinokitiol | *S. aureus* | | | [102] |
| | Covalent immobilization with PDA | PEEK | K-12 (antimicrobial peptide) | | *S. aureus* | | [85] |
| | Combination of UV-graft polymerization and wet chemical method | Acrylic acid graft polymerization on PEEK | Chitosan | | *E. coli* | | [45] |
| | Dripping | CMC[a] grafted Carbon fiber reinforced PEEK/nano hydroxyapatite composite | Bone forming peptide | | | *S. aureus* | [101] |
| | Absorption | $TiO_2$/ZnO coated PEEK | Vancomycin salt | *E. coli* | | *S. aureus* | [76] |

(Continued.)

**Table 2.** (Continued.)

| | Modification method | Substrate | Material | High (Bacterial effect > 80%) | Moderate (Bacterial effect between 80%–50%) | Low (Bacterial effect < 50%) | Reference |
|---|---|---|---|---|---|---|---|
| | Absorption | $TiO_2$/ZnO coated PEEK | Ampicillin salt | *S. aureus* | *E. coli* | | [76] |
| | Absorption | $TiO_2$/ZnO coated PEEK | Ampicillin (50% w/v) and vancomycin (50% w/v) salt mixture | | *S. aureus* | *E. coli* | [76] |
| | Reaction with mixing | PEEK | Quaternary ammonium salts | *S. aureus* | *E. coli* | | [103] |
| | UV photoinsertion grafting | PEEK | Modified PEG[b] and quaternized poly(dimethy laminoethyl acrylate) | *S. aureus* | *E. coli* | | [104] |
| Ions, Functional groups, Nanoparticles | Soaking in Tollens' reagent and reduction of $[Ag(NH_3)_2]^+$ | PDA[a] coated PEEK | Ag nanoparticles | *E. coli, S. aureus* | | | [97] |
| | Immersion in $MnCl_2$ and $CuCl_2$ solutions | PDA[a] coated PEEK | $Mn^{2+}$ (4.52 μg $ml^{-1}$: release concentration in 24 h) and $Cu^{2+}$ (6.58 μg $ml^{-1}$: release concentration in 24 h) ions | *S. aureus, E. coli* | | | [65] |
| | Sulfonation reaction | Sulfonated PEEK (13.47 wt. %) | $SO_3H$ | *S. aureus, E. coli* | | | [99] |
| | Schiff base reaction between the keto carbonyl group and EDA[c] in PEEK | Sulfric and nitric acid mixture (1:1) treated PEEK | Amino groups ($-NH_2$) and $NO_2$ groups (13.69 wt.% N) | *S. aureus, E. coli* | | | [84] |
| | Immersion | Acrylic acid graft polymerization on PEEK | $Zn^{2+}$ ions | | *S. aureus* | | [105] |
| | Cold plasma treatment with $N_2$ | PEEK | N containing functional groups | | | *S. mutans, S. aureus* | [60] |
| | Immersion and sonication | PEEK | $SO_3H$ | | | *S. aureus, E. coli* | [50] |
| | Magnetron sputtering | Sulfonated PEEK | Cu nanoparticles (1.40 at. %) | *MRSA* (Adherent) | *MRSA* (Planktonic) | | [62] |
| | Immersion in 0.05%w/v GO solution | Sulfonated PEEK | GO | | *E. coli* | *S. aureus* | [106] |

(Continued.)

**Table 2.** (Continued.)

| | | | | | | |
|---|---|---|---|---|---|---|
| | Immersion in HF | PEEK treated with argon plasma immersion ion implantation | F | *P. gingivalis* | | [107] |
| | Plasma immersion ion implantation | Carbon fiber reinforced PEEK (2 h of implementation) | $ZrO_2$ | *S. aureus* | *E. coli* | [93] |
| | *In situ* growth method | Sulfonated PEEK | Zeolitic imidazolate framework-8 (ZIF-8) | *E. coli, S. aureus* | | [108] |
| | *In situ* growth method/self-assembly ($Ag^+$ loading (1 mM $AgNO_3$)) | Sulfonated PEEK | ZIF-8 | *S. aureus, E. coli* | | [108] |
| Combination of polymers, drugs and nano-particles | Immersion and covalent grafting | Sulfonated PEEK | GO, PDA nanolayer and bone forming peptide | *S. aureus, E. coli* (808 nm NIR[d]) | | [109] |
| | Spinning | Dopamine coated sulfonated PEEK | μCuO/nAg in silk fibroin solution | *S. aureus, E. coli* (at pH 5) | *E. coli* (at pH 7.4) | [98] |

[a] Carboxymethyl chitosan.
[b] Polyethylene glycol.
[c] Ethylenediamine.
[d] Near infrared.

According to the study of Ouyang *et al*, the hydrothermal treatment of sulfonated PEEK samples decreased the sulfur content and antibacterial efficiency of *E. coli* [99]. For example, when the sulfur content was decreased from 13.47 wt. % to 0.74 wt. %, the antibacterial efficiency was decreased from 100% to 24% [99].

On the other hand, no change in antibacterial rate was observed for *S. aureus; it* stayed at 100% [99]. The difference between the antibacterial rates of *E. coli* and *S. aureus* stemmed from the different pH endurance of the two bacteria. Since *E. coli* produced gaseous ammonia during the transfer of *Gln* to *Glu*, neutralization of protons occurred in the acidic environment, and intracellular pH was increased [99]. On the contrary, *S. aureus* can endure a pH between 4.0 and 7.0 [99]. Another reason for the different antibacterial efficiency was the morphology of the two bacteria. *E. coli* is rod-shaped with 1 μm of diameter and can not be trapped on the porous surface of sulfonated PEEK [99]. Conversely, *S. aureus* has a spherical shape with a diameter of 0.5 μm and can be trapped easily in the pores of the sulfonated samples [99].

*4.1.2. Ion immobilization*

Some elements such as Ag, Cu, and Zn show antibacterial effects when coated, mixed to form a PEEK nanocomposite, or immobilized on the surface of the PEEK. Zn-doped samples increased the antibacterial efficiency by destroying bacterial nucleic acids, DNA, and RNA synthesis. It penetrates the cell wall and reacts with $-SH-$, $-NH2_2$ groups [105]. The antibacterial effect of $Cu^{2+}$ ions was studied on the sulfonated PEEK samples. Trap killing and contact killing were the mechanisms of bacterial inhibition [62]. *In vivo* studies showed 97% improvement in antibacterial effectiveness by incorporating $Cu^{2+}$ ions with 1.40 at. % [62]. Fluoride (F) is another element immobilized on the PEEK surface. Argon plasma immersion ion implantation technique was applied to increase its immobilization efficiency. The mechanism of F on the antibacterial property of PEEK was explained by the inhibition of proton-translocating $F^-$ATPases [107].

A study on the antibacterial ability of ZIF-8 showed that it had an excellent loading capacity of $Ag^+$ ions with a steady release behavior.

Moreover, the gradual degradation of ZIF-8 occurred in an aqueous environment due to the hydration-deprotonation released $Zn^{2+}$ ions, which improved the antibacterial property [108].

#### 4.1.3. Graphene oxide immobilization

GO is a carbon-based compound with functional groups such as hydroxyl, epoxy, carboxyl, carbonyl, phenol, lactone, and quinone [114]. GO immobilization on sulfonated PEEK increased the antibacterial effect against *E. coli* [106]. The mechanisms proposed for affecting *E. coli* were explained by acid endurance, shape, membrane structure, and oxidative stress caused by ROS [106]. First, GO neutralizes the surface of PEEK, which decreases the number of *E. coli* since *E. coli* has mechanisms for acid resistance. Secondly, *E. coli* has a rod-like shape with a diameter of about 1 μm, which the sharp edges of GO can easily deform. A thin peptidoglycan membrane of *E. coli* results in a decrease in its survival rate. The other mechanism was related to ROS. GO generates ROS production that causes oxidative stress. Oxidative stress results in rupture, mutation, and change in the thermal stability of DNA [106].

#### 4.1.4. Drug immobilization

Immobilizing the drugs onto the coatings of PEEK or sulfonated PEEK samples is another technique to gain antibacterial properties. Moxifloxacin hydrochloride is a drug that inhibits DNA gyrase and topoisomerase IV and blocks DNA replication [50]. Although PEEK had no antibacterial effect, the release of moxifloxacin hydrochloride coated on PEEK increased the antibacterial effect by about 100% [50]. Vancomycin and Amphicilin are the antibiotics used to improve the antibacterial properties of PEEK. Vancomycin improved antibacterial results for *S. aureus*, whereas Amphicilin was a good inhibitor of *E. coli* [76]. An antimicrobial peptide recombinant mouse beta-defensin- 14 was used to improve the antibacterial property of PEEK. It has a broad spectrum of antibiotic activity, encompassing gram-positive, gram-negative, fungi, viruses, and multi-drug resistant bacteria. It avoids immune system responses since it has a biological origin [58]. Hinokitiol is another compound with a natural origin and has antiviral, antibacterial, antifungal, antitumor, and insecticidal properties without cytotoxic effects [102]. Hinokitiol loaded on PEEK showed excellent antibacterial properties due to its slow release. The antibacterial mechanism of hinokitiol was explained by the degeneration of proteins in the bacterial membrane [102].

Mino is another antibacterial drug that breaks the association of aminoacyl-tRNA and bacterial ribosome and disintegrates bacterial cells [47]. Minocycline-loaded liposomes were immobilized on the PEEK surface to increase the antibacterial effect against *S. mutans* and *P. gingivalis* [47].

The effect of berberine as an antibacterial agent was investigated *in vivo* [61]. The berberine was adsorped on sulfonated PEEK functionalized with osthole nanoparticles (an extract of cnidium fruit that supports osteogenesis). The results showed that severe edema around PEEK implants was observed without berberine at the end of the second week [61]. Additionally, severe osteomyelitis was detected at the end of the fifth week [61]. A high degree of inflammatory hyperplastic tissue was formed around the femoral condyle, and displacement of the implants occurred [61]. On the other hand, no inflammatory response was detected for berberine-containing samples that supported collagen formation and were tightly wrapped with bone collagen [61].

Genistein is a phytoestrogen molecule extracted from soy products. It is a good antioxidant, anti-inflammatory, antimicrobial, and anti-carcinogenic compound, showing good biocompatibility. In a study, 40 vol. % Ta and PEEK sulfonated composites loaded with genistein showed a bacteriostatic rate above 97%. Unloaded samples showed a bacteriostatic rate of 68.37% for *S. aureus* and 61.02% for *E. coli* [100]. Similarly, genistein loading on tantalum pentoxide and PEEK composites increased the antibacterial rate from 90.27% to 100% for *E. coli* and 88.27% to 100% for *S. aureus* after sulfonation [115]. Salts of vancomycin and ampicillin combination was loaded on PEEK to obtain antibacterial property [76].

#### 4.1.5. Immobilization with graft polymerization

UV-induced graft polymerization technique was used to introduce carboxylic groups on the surface of PEEK [45]. Acrylic acid was used as a source of the functional groups [45]. The amino groups of chitosan were attached by wet chemical methods after the carboxyl groups were formed. Presenting carboxyl groups onto the surface of PEEK increased the chitosan grafting degree by 1.4% [45]. Polystyrene sulfonate was another compound that was immobilized onto PEEK by UV. After one day of incubation, a significant decrease was observed against *E. coli, S. aureus,* and *P. gingivalis* for grafted samples [116].

Another study grafted PEG as an antifouling agent and quaternized poly(dimethylaminoethyl acrylate) as a bactericidal on the PEEK surface. As the molecular weight of PEG was increased, the hydrophilicity increased, whereas protein adsorption decreased. These changes resulted in the inhibition of cell attachment [104]. The synergistic effect of the bactericidal and antifouling parts was only achieved after PEG grafting with Mn:2000 g $mol^{-1}$ as short quaternized poly(dimethylaminoethyl acrylate) chains exposed to the bacterial suspension [104]. PEG with higher molecular weight caused steric hindrance and the interaction between the bacterial wall and quaternized poly(dimethylaminoethyl acrylate) was inhibited by larger-sized PEG chains [104].

### 4.2. Coating with an antibacterial material

Coating PEEK with an antibacterial material is the second mainly studied method to improve the antibacterial property of PEEK. Coating techniques are separated into two: self-assembly and classical methods. The details of the coating methods applied to enhance the antibacterial properties of PEEK are summarized in table 3, with their advantages and disadvantages. The layer-by-layer self-assembly coating examples were Zn/chitosan, Ag/alginate, and brushite/gentamicin surface (figure 3). In the layer-by-layer self-assembly technique, the generation of charges between the solution and coated layer resulted in a coating of another layer [75, 117]. Surface modifications such as sulfonation or application of an adhesive coating with polyethyleneimine [118] and polystyrene sulfonate were used to overcome the chemical inertness of the PEEK surface. Polydopamine is another compound that is widely used to form an adhesive interlayer with its large amount of free catechol groups [89]. Classical methods for coating PEEK are immersion, dip coating, precipitation, vapor deposition, magnetron sputtering, and radio-frequency co-sputtering [44, 53, 55, 56, 119–126]. There are examples of coating with one element, such as $Ag^{+}$, $Cu^{2+}$, $Mg^{2+}$, red selenium, and gray selenium, and dual systems, such as hydroxyapatite with the combination of drugs, GelMA, sodium butyrate and hydrogels combined with bone-forming peptides and chlorogenic acid (figure 3). Since immersion and dip coating methods are easy and cost-effective, they are frequently preferred for coating.

The antibacterial studies of coated PEEK with different techniques and materials are listed in table 4. According to table 4, the coating systems composed of two or more agents are more pronounced. The materials in those systems have been chosen to simultaneously increase osteogenic and antibacterial abilities.

In most of the studies using the coating process to increase the antibacterial response of PEEK, osteogenic properties and biocompatibility were investigated [52, 55, 56, 59, 68, 80, 119, 128, 133, 135]. The coating of ZnO/Ag nanoparticles on PEEK showed elongated and overlapped lamellipodia in MG-63 cells, which was the indicator of healthy cells. Compared to Ag-decorated samples, enhanced cell spreading, proliferation, alkaline phosphatase activity, and osteogenesis-related genetic expression results were obtained [117]. Layer-by-layer coated brushite/gentamycin sulfate on PEEK gave acceptable biocompatibility results *in vitro* on MG-63 cells. Osseointegration ability in bone healing was detected *In vivo* experiments for the samples with 6 layers [75]. In another study, a coating system that incorporated Cu into a PDA adhesive layer was produced. The osteogenetic activity of rBMSCs was measured, and angiogenesis was measured using a Matri-gel tube-forming assay using HUVEC cells. Both parameters gave superior results [126]. Moreover, illumination-sensitive and pH-sensitive systems target antibacterial and osteogenic abilities at the same time. The systems with PDA-wrapped zeolitic imidazolate framework-8, $(CuFe_2O_4)$/GO and black tantalic oxide resulted in hypothermia and ROS generation at 808 nm NIR illumination [57, 120, 135]. The pH-responsive system included copper citrate. The release of copper increased as the pH of the environment decreased. Copper release elevated the cell structure's copper content, producing ROS and damaging protein [137]. In another study, Ag nanoparticles were trapped in PDA layers. As pH decreased, $Ag^{+}$ ion release started, and bacterial infection occurred [138].

Bioactivity is another parameter that shows the success of the implant. Formation of the apatite structure on the surface of bone implants increases the sites for the cells to attach, proliferate, differentiate, and adsorption of proteins. The multi-layer coatings with bioglass 45S5/PEEK composite at the lower layer and silver nanoclusters/silica composite at the upper layer showed apatite-like crystals formation due to bioglass incorporation [125]. In another study, nanoporous magnesium calcium silicate was coated on PEEK with a melting method. Compared with uncoated PEEK, better apatite mineralization in simulated body fluid was observed in coated samples [134]. The coating system, including PDA, nanohydroxyapatite, and lysozyme on PEEK, showed apatite-like deposits in simulated body fluid. The phenol groups in PDA impacted the biomineralization [89].

Wear properties gain importance, especially in artificial joint implants. Coating of the implant is a solution to add a wear resistance property to the material. In a study in which hard TaN-(Ag, Cu) nanocomposite films were applied on PEEK, frictional forces and wear rate decreased after annealing since Ag and Cu particles acted as solid lubricants [122].

Adhesion properties of the coating material should be investigated for coated biomaterials. The formation of the cracks on the coating material forms potential sites for bacterial growth. In a study, a multi-layer coating composed of Ag nanoparticles, silica, bioglass 45S5, and PEEK was produced by a radio-frequency co-sputtering method with a sputtering time of 15 min. Good adhesion properties were obtained with second critical load values between 17.60 and 12.82 N [125].

In recent studies, two or more constituents have been added to the coating material to enhance various properties of substrate PEEK. Adding an antibacterial ion such as $Ag^{+}$ was a common technique used for this purpose, whereas, in some studies, more than one antibacterial constituent was used. For example, the study aimed at coating PEEK with Ag-doped trimagnesium phosphate hydrate showed antibacterial properties depending on Ag concentration. Without Ag, no antibacterial property was mentioned [139].

**Table 3.** Coating techniques used to improve antiacterial properties of PEEK.

| Coating technique | Working principle | Pros | Cons | Reference |
|---|---|---|---|---|
| Immersion and dip coating | Immersing the material into the coating solution in a specified time and concentration. | - Easy to apply<br>- Variety of materials can be coated with this method.<br>- Not limited to line of site. | Coating thickness is less controllable | [52, 55, 56, 68, 80, 123, 127] |
| Chemical Vapor Deposition | Solid precursor is vaporised and deposited on the substrate. | - low temperature (∼75 °C in ICPECVP[a])<br>- fast deposition rate (ICPECVP)<br>- Good coverage (ICPECVP)<br>- Not limited to line of site. | - High temperature (∼230 °C) results in degradation due to stress formation.<br>- Vacuum is required.<br>- Coating thickness ∼500 nm can be obtained. | [121, 128] |
| Magnetron Sputtering | Ar ions accelerated and the target surface is bombarded to eject target atoms. The ejected target atoms are condensed on the substrate. | - Very high controllable coating thickness (∼3 nm) can be obtained.<br>- High-speed<br>- low-temperature<br>- deposition<br>- Uniform and strong adhesion<br>- Low damage rates | - High cost<br>- Low metal ionization rate<br>- Non-uniform etching between the targets causes inhomogeneous film thickness and low reproducibility of films. | [3] |
| Precipitation | The conversion of solutions into insoluble solid particles on a substrate occurs after a reaction between salt solutions in a controlled pH. | - Low cost<br>- Easy to apply | - Large amount of solutions are required.<br>- The coating thickness and particle size are less controllable<br>- The methods of elimination of substrate from remaining solutions are time consuming. | [53] |
| Electrophoretic deposition | Charged colloidal particles in a liquid medium are collected on an electrically conductive substrate by applying an electrical field. | - Low cost and simple apparatus<br>- Not limited to line of site.<br>- Low temperature process<br>- High-speed | - High electrical conductivity is required for the substrate material.<br>- Poor adhesion | [129] |

(Continued.)

**Table 3.** (Continued.)

| | | | | |
|---|---|---|---|---|
| Radio frequency co-sputtering | High voltage alternating current power force sends radio waves through a vacuum chamber and creates a positively charged sputtered gas ($Ar^+$) to hit the target coating material. The ejected atoms are condensed on the substrate. | - Any solid material can be coated.<br>- High density, high purity in films<br>- Strong film adhesion to the substrate | - Expensive<br>- Requires high power to supply radio frequency<br>- High electromagnetic radiation | [44] |
| Layer by layer self assembly | | - Provide a controlled and sustained release<br>- Combining different materials in separate layers. | - Applied only for charged solutions | [117] |

[a] ICPECVD: inductively coupled plasma-enhanced chemical vapor deposition.

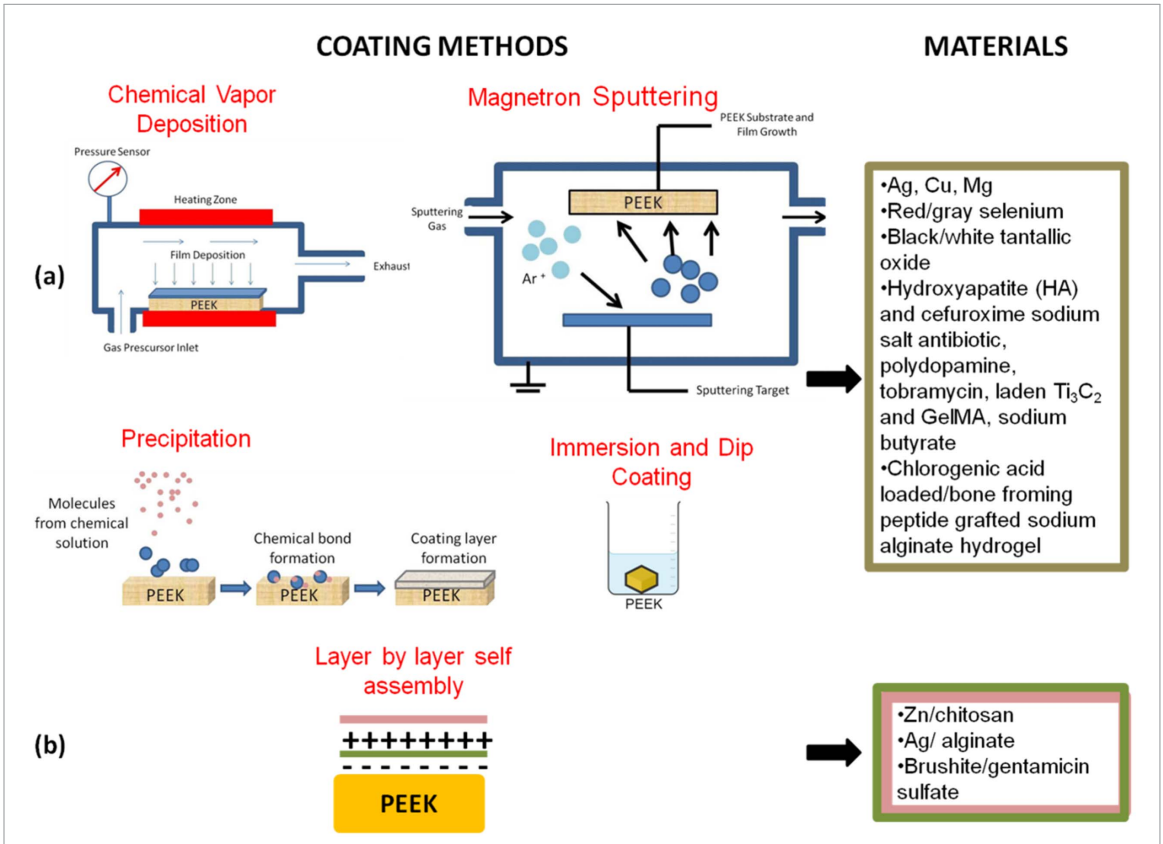


**Figure 3.** Coating methods and materials to improve the antibacterial properties of PEEK; (a) Classical methods: immersion, dip-coating, precipitation, vapor deposition, magnetron sputtering and radio-frequency co-sputtering with studies containing one element such as $Ag^+$, $Cu^{2+}$, $Mg^{2+}$, red/gray selenium, black/white tantalic oxide and dual systems such as hydroxyapatite with combination of drugs, GelMA, sodium butyrate and hydrogels combined with bone forming peptides and chlorogenic acid [44, 53, 55, 56, 119, 121–126]; (b) Layer by layer self-assembly: generation of charges on the surface with examples of dual systems such as Zn/citosan, Ag/alginate and brushite/gentamicin sulfate [75, 117]. The figures that represent chemical vapor deposition, magnetron sputtering and precipitation are adapted from [130–132], respectively with permission. Adapted from [130] with permission from the Royal Society of Chemistry. Adapted from [131]. CC BY 3.0. Adpated from [132]. CC BY 4.0.

Similarly, in the study which combined gelatin and vancomycin as a composite coating on PEEK, the gelatin increased the number of colonies without vancomycin [80].

Among the studies, Ag-included coatings gave highly effective results in terms of antibacterial properties [3, 52, 117]. Tantallic oxide was used in coating and composite forms in the studies. The

**Table 4.** The antibacterial effect of the modification with coating with an antibacterial material.

| | Material | Coating method | High (Bacterial effect > 80%) | Moderate (Bacterial effect between 80%–50%) | Low (Bacterial effect < 50%) | Reference |
|---|---|---|---|---|---|---|
| Drugs, Peptides, Proteins and Polymers | PDA | Dip coating | | *S.aureus* | *E.coli* | [97] |
| | Chlorogenic acid (4 mg ml$^{-1}$) loaded/bone forming peptide grafted sodium alginate hydrogel | Immersion | *S. aureus, E. coli* | | | [123] |
| | Vancomycin gelatin nanoparticles | Immersion and using PDA as an adhesion agent | *S. aureus, S. mutans* | | | [80] |
| | GS | Immersion and using PDA as an adhesion agent | *S. aureus, E. coli* | | | [127] |
| Ions, Functional groups, Nanoparticles | TaN-(Ag, Cu (7 at. %)) | Reactive co-sputtering and rapid thermal annealing | *S. aureus, E. coli* | | | [122] |
| | Cu/C:F[a] | GAS[b] deposition and Radio frequency magnetron sputtering | *E. coli* | | | [44] |
| | Mg (high purity) | Vapor deposition | *S. aureus* | | | [121] |
| | Ag nanoparticles (12 nm coating thickness) | Magnetron sputtering | *S. aureus, S. mutans* | | | [3] |
| | Red selenium nanoparticles | Precipitation method | | | *P. aeruginosa* | [53] |
| | Gray selenium nanorods | Precipitation method with 6 d of heat treatment (at 100 °C) | | | *P. aeruginosa* | [53] |
| | Black tantalic oxide submicron particles | Immersion and using PDA as an adhesion agent | *S. aureus, E. coli* (under NIR[c] irradiation) | | | [120] |
| | White tantalic oxide | Immersion and using PDA as an adhesion agent | | | *S. aureus, E. coli* (under NIR[c] irradiation) | [120] |
| | Cu II (concentration: 10 μg ml$^{-1}$) | Immersion and using PDA as an adhesion agent | | *MRSA* | | [126] |
| | ZnO/GO | Dip coating | *S. sanguinis, P. gingivalis* | | *F. nucleatum* | [68] |

(Continued.)

**Table 4.** (Continued.)

| | | | | | | |
|---|---|---|---|---|---|---|
| | Silicon nitride | Inductively coupled plasma-enhanced chemical vapor deposition | *S. aureus, E. coli* | | | [128] |
| | GO | Immersion after sulfonation of PEEK | *P. gingivalis* | *S. mutans* | | [59] |
| | $TiO_2$ | Immersion after coated with PDA | *S. aureus, S. mutans* | | | [133] |
| | Nano magnesium silicate | Immersion | | *E. coli* | *S. aureus* | [134] |
| | $(CuFe_2O_4)$/ GO | Immersion after coated with PDA | *S. aureus, E. coli* | | | [57] |
| Combination of polymers, drugs and nanoparticles | Ag alginate (1.36 at. %) /Zn chitosan (0.69 at. %) dual layer | Layer by layer self assembly | *S. aureus, E. coli* | | | [117] |
| | Brushite containing GS (>10 μg) | Layer by layer deposition by immersion | *S. aureus, E. coli* | | | [75] |
| | Ag nanoparticles (AgNPs) incorporated silk fibroin (SF)/GS | Immersion (AgNPs) and dripping (GS) | *S. aureus, E. coli* | | | [52] |
| | Nano magnesium silicate loaded with Genistein and Curcumin | Immersion | *S. aureus, E. coli* | | | [134] |
| | PDA-wrapped Zeolitic imidazolate framework-8 (ZIF-8) | Immersion | *S. aureus, E. coli* (under NIR[c] irradiation) | | | [135] |
| | Stearyltrimethy lammonium chloride-modified HA | Electrophoretic deposition | *S. aureus* | *E. coli* | | [129] |
| | 95% $TiO_2$ (doped with 10 x silver carboxylate)-5% PDMS | Dip-coating | *S. marcescens* | | | [136] |
| | Vancomycin loaded PLGA[d]-PEG-PLGA[d] hydrogel | Immersion | *MRSA* | | | [81] |
| | Lysozyme on PDA-nano HA composite | Immersion | *S. aureus, E. coli* | | | [89] |

[a] Cu deposition was applied for 2 min and C:F thickness was 10 nm.

[b] GAS deposition: Haberland-type gas aggregation source was used to deposit Cu nanoparticles.

[c] Near-infrared.

[d] Poly($_{D,L}$-lactic acid-co-glycolic acid).

antibacterial properties were less pronounced in the composite form and without NIR. In the coating form, black tantallic oxide showed an antibacterial ratio higher than 90% under NIR illumination [120]. On the other hand, white tantallic oxide results stayed at a ratio lower than 50% [120]. Black tantallic oxide was the processed version of white tantallic oxide. Structural defects and oxygen vacancies were produced on white tantallic oxide with the magnesium thermal reduction method. Unlike white tantallic oxide, black tantallic oxide had high photothermal effects, increasing the local temperature under NIR and killing the bacteria [120]. Compared to other metallic nanoparticles, selenium gave less effective results [53]. The biofilm formation could not be prevented entirely and increased in three days, however, the density of *P. aeruginosa* decreased in grey and red selenium-coated samples compared to uncoated PEEK [53]. Loading antibacterial drugs or compounds in the coating has been an effective solution to increase the antibacterial properties of PEEK. For example, the slow release of curcumin (65.17% of curcumin was released in 336 h) reduced the amount of *E. coli* from 54.87% to 98.59% and *S. aureus* from 48.71% to 99.62% [134].

The responses to the coating material changed according to the type of bacteria. It was shown that ZnO/GO coatings on PEEK gave higher antibacterial rates against initial colonizer *S. sanguinis* (∼97%) and late colonizer *P.gingivalis* (∼89%) [68]. On the other hand, middle-stage colonizer *F. nucleatum* was affected less compared to the initial and late stage colonizer examples. Therefore, it was important to study the effects on *S. sanguinis* and *P.gingivalis* in the biomaterials studies for dental applications [68].

#### *4.2.1. Coating with ions*

Silver, copper, and zinc are antibacterial ions directly coated or incorporated into the coating material. Silver-containing coatings possessed cytotoxicity when the percentage of silver in the compound was 0.21 wt. % [140]. The thickness of the coating of Ag nanoparticles is another important parameter for the antibacterial property. For example, 3 nm of coating showed 99.4% and 99.7% antibacterial rates against *S. mutans* and *S. aureus*, respectively [3]. When the thickness was increased to 9 nm, a 100% antibacterial effect against the two bacteria species was observed [3]. The number of adhered colonies was consistent with the antibacterial rate results [3]. $Ag^{+}$ doping is another technique to provide $Ag^{+}$ ion release. An $Ag^{+}$ doped $TiO_2$/PDMS hybrid coating was produced for antibacterial purposes [48]. As the $Ag^{+}$ doping amount was increased in the coating, the optical density, the indicator of *S. aureus* bacterial concentration, decreased [48]. The release of $Ag^{+}$ ions was dependent on the $TiO_2$/PDMS content. The total inhibition was seen at 38.4 µl of Ag [48]. *S. epidemidis* was more sensitive than *S. aureus*. Total inhibition was seen at the same Ag concentration (38.4 µl). However, the optical density values dramatically decreased even at a doping volume of 2 µl [48]. A sustained release was obtained for the study with between 58% and 65% release of Ag at the end of the 1000th hour. When the amount was reduced by 10 fold, the release amount decreased to between 7% and 10%. The initial burst was seen in the first 150 h [48]. In another study, PDA was used as a carrier material of Ag and coated on PEEK [97]. A release profile with an Ag amount between 5% and 10% was seen in 20 d. Additionally, this study showed that the initial burst of Ag inhibited MC3T3-E1 cells in first 3 d [97]. Therefore, the addition amount should be adjusted to so that it should not cause cytotoxicity. The carrier material and antibacterial agent also define the release profile. In a study, cefuroxime sodium salt antibiotic loaded on hydroxyapatite and a burst release resulted in a release amount between 86.1% and 96% in 24 h [141]. The high porosity of the carrier and weak bonds between the antibacterial agent and carrier resulted in a high initial burst. Similarly, the coating of gentamycin sulfhate-loaded brushite on PEEK lost all gentamycin sulphate before 72 h [75]. Moreover, the antibacterial agent form is important. The salt form of cefuroxime was not chemically stable and suggested to be used by local systems [141].

In another study [44], the antibacterial effect of Cu nanoparticles was screened by C:F thin film, a thin layer used to stabilize Cu nanoparticles on the surface of the PEEK. The Cu layer was washed away without the C:F thin film. On the other hand, 40 nm of thickness resulted in a bacteriostatic surface without reduction of bacterial growth [44]. The optimum C:F film thickness was 10 nm, which enabled the stabilization of Cu nanoparticles and water penetration into the Cu layer [44]. The water penetration led to the dissolution of $Cu^{2+}$ ions and the initiation of the antibacterial effect.

$Mg^{2+}$ is another ion that is used for obtaining antibacterial PEEK. Highly pure Mg was coated on PEEK with the vapor deposition technique. In 21 d, Mg coating degraded with an effect of 99% antibacterial rate on *S. aureus*. The mechanism of bacterial inhibition was explained by strong alkali environment formation by releasing $Mg^{2+}$ ions [121].

The processing parameters affected the antibacterial property. In a study investigating the dual ion incorporation as a coating material, Ag and Cu particles were nucleated and grown on the TaN matrix using rapid thermal annealing at 200 °C [122]. As the annealing time increased to 8 min, the antibacterial efficiency increased from ∼55% to 70% and ∼60%–80% for *S. aureus* and *E. coli*, respectively (the deposition was 2 at. %) [122]. The augmented number of Ag and Cu particles on the surface with annealing time explained the improved antibacterial property. $Ag^{+}$ and $Cu^{2+}$ ions destroyed the bacterial membrane. It was also inferred that *E. coli* was

affected more than *S. aureus* due to their high sensitivity to $Ag^{+}$ ions appearing on the surface more quickly than $Cu^{2+}$ ions [122]. In another system, dual-metal-organic frameworks were used as an antibacterial coating for PEEK [74]. Besides its drug carrier ability, it released metal ions ($Zn^{2+}$ and $Mg^{2+}$) and 2,5-dihydroxyterephthalic acid, increasing the pH and forming an alkali environment on the surface. The increase in pH reached 8.4 in 24 h, which inhibited bacteria with about 100% efficiency [74].

*4.2.2. Coating with a drug carrier material*

The antibacterial effect can be provided by coating with a carrier of an antibacterial drug. For example, antibiotics can be loaded on coating materials such as HA. In a study [141], HA showed no antibacterial properties compared to the control unless cefuroxime sodium salt antibiotic was loaded. Another antibiotic coated on PEEK was GS. It was a broad-spectrum antibiotic with low toxicity for the human body. GS was coated on PEEK by mixing with a ceramic material, brushite [75]. According to the fluorescence spectrophotometer measurement at 340 nm, the release amounts of GS from the coating system were detected as >10 μg, >60 μg, and >100 μg in simulated body fluid. These release amounts resulted in 100% inhibition of *S. aureus* up to day 5. The antibacterial coating started to lose its activity after the fourth day [75]. Silk was another alternative to obtain a sustained release of gentamicin. When the combination was coated on $SrCO_3$-PDA-modified PEEK, it significantly improved the antibacterial effect of PEEK and sulfonated PEEK [142]. Nano magnesium silicate was an alternative bioactive ceramic material to load a natural antibacterial compound, curcumin [134]. Similarly, tobramycin, an antibacterial drug, was used to gain antibacterial properties in PEEK samples. The antibacterial mechanism of tobramycin was explained as preventing the translation from mRNA into protein. Modification of the PEEK samples by combining tobramycin with GelMA increased osteogenicity. Tobramycin screened the bacterial viability effect of GelMA [55].

Butyrate, a fermentation product of gut microbiota, possessed anti-inflammatory, antimicrobial, and immunomodulatory properties. Sodium butyrate increases the phagocytic activity of macrophages by improving the release of ROS [56]. Chlorogenic acid is another compound that has antioxidant and anti-inflammatory effects. It has been used in a sodium alginate hydrogel system with a combination of bone formin peptides [123]. Coating PEEK with crosslinked benzophenone-substituted hydrogel showed up to log5 fold effective against *MRSA* and *E.coli*. Therefore, biofilm formation was significantly reduced. Benzophenone is used to design anti-adhesive and antimicrobial surfaces with improved cell viability [143]. In another study, a traditional Chinese medicine-inspired compound, total alkaloids from Semen Strychnine (TASS), was used to enhance antibacterial properties. The bacterial inhibition rate against *S. aureus* and *E. coli* increased with TASS content. TASS had healing effects on antiinflammation and analgesia, according to the *in vivo* studies [144]. A mouse ear swelling test was applied to detect the antiinflammation by weighing the control group and samples after the treatment [145]. The analgesic effect was observed by the formalin test. Formalin solution was injected into drug-treated mice, and their reactions were graded after 10, 30, 60, and 90 min [145].

Polyvinyl alcohol (PVA) and PLGA were two polymers used as drug carriers coated on sulfonated PEEK by cyclic freezing and thawing. The initial burst of vancomycin hydrochloride-loaded PVA increased antibacterial activity, whereas the sustained release of Dexamethasone-loaded PLGA enhanced osseointegration [146]. In another study, PLGA was used to trap vancomycin and ampicillin salts to obtain *S. aureus* bacterial inhibition by over 40% in 30 d [147].

*4.2.3. Coating with oxides*

Coating with oxides gained importance in photothermal therapy. They showed antibacterial properties with near-infrared irradiation. Black bioactive materials became popular due to photothermal therapy. They can transform the energy of near-infrared light into heat energy. Therefore, photothermal therapy has proposed a solution for bacterial destruction. Black tantalic oxide coating on PEEK showed considerable antibacterial properties with NIR irradiation [120]. A bone channel with a 1.5 mm diameter was formed at the femur of rat samples. The specified amount of *S. aureus* suspension was injected, and sterilized samples were implanted into the bone channel. NIR irritation was prolonged for 5 min to three days. A thermal imager was used to detect the temperature changes. The implanted samples were removed after 14 d, and the bacteria on the surface of the implanted samples were collected by ultrasonic vibration. The specified amount of diluted bacterial suspension was spread onto the agar plate and incubated at 37 °C for one day. *In vivo* studies showed that the temperature increased to 51.8 °C in black tantalic oxide-coated PEEK with NIR irradiation. The corresponding antibacterial rate was 93.1% [120]. Copper ferrite ($CuFe_2O_4$)/GO is another coating material showing strong antibacterial properties after photoactivation. The antibacterial property was provided by localized hypothermia and ROS generation at 808 nm NIR illumination. GO addition increased the antibacterial rate from 83.85% to 99.94% against *S.aureus* and 76.43% to 99.57% against *E.coli* [57]. In another study, CuS/GO system was used to obtain antibacterial efficiency under NIR at 808 nm. The local temperature increased to 58.4 °C around the material subcutaneously implanted in mice. *In vivo*

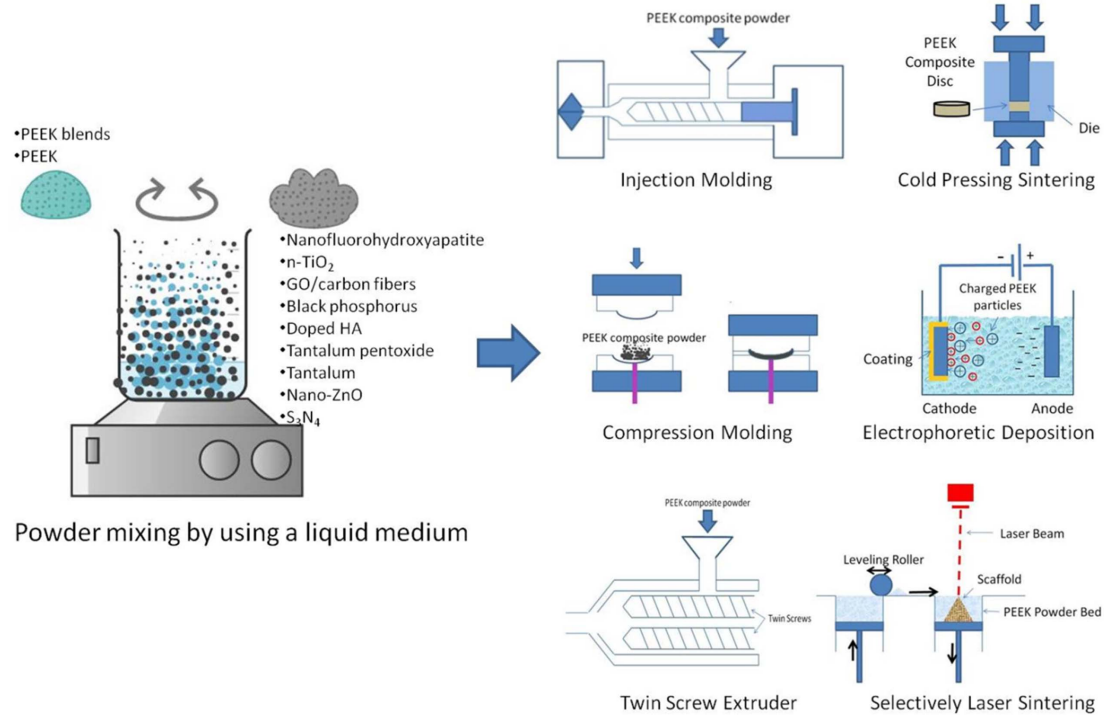


**Figure 4.** Composite production to obtain antibacterial PEEK consists of two steps in most studies. The first step includes powder mixing using a liquid medium such as ethanol to obtain a homogeneous mixture. PEEK powder or blends of PEEK and reinforcements in powder form are dispersed in the medium [92]. The second step includes heating above the melting temperature (PEEK melting temperature: ∼343 °C) for injection molding, compression molding, selectively laser sintering, cold pressing sintering, and twin-screw extrusion [51, 54, 144, 149, 150] to obtain composite materials or electrophoretic deposition for composite coatings [83]. The figures that represent injection molding [151], swin screw extruder [151] and selectively laser sintering [152] are adapted with permission. Cold pressing sintering figure is reprinted (adapted) with permission from [153]. Copyright 2018 American Chemical Society. Adapted from [151]. CC BY 4.0. Adapted with permission from [153]. Copyright (2018) American Chemical Society. Adapted from [152]. CC BY 4.0. Adapted from [151]. CC BY 4.0.

antibacterial efficiency against S. *aureus* was detected as 99.9% after applying NIR at 808 nm for 10 min in samples with glucose oxidase immobilization after being coated with PDA/CuS/GO [148]. GO and bone-forming protein immobilized surface of PEEK showed an improved antibacterial effect after treating with NIR at 808 nm for 10 min. The antibacterial rate reached ∼97.55% and ∼90.57% against *S. aureus* and *E. coli*, respectively [109].

### 4.3. Composites with antibacterial properties

Forming composites is another method to improve the antibacterial properties of PEEK. Ceramics are the most common reinforcement materials used in the studies. In addition to ceramics, organic compounds such as gelatin, drugs such as lactam, and total alkaloids have been studied (figure 4). Table 5 lists the composite materials with their antibacterial effects on PEEK.

In some of the studies, it was reported that the reaction of bacteria changed according to their types. For example, a study that investigated the antibacterial properties of (GO), carbon fibers, and PEEK composite on Ti-6Al-4 V showed that the cell membrane structure defined the antibacterial properties. Graphene oxide showed a nano-blade effect and concurrently resulted in the chemical extraction of cell membrane lipids concurrently. Compared to Gram-negative *E. coli* (with a membrane consisting of a thin peptidoglycan layer and an outer lipid membrane) and Gram-positive *S. mutans* with a thick capsule, *S. aureus* (with a membrane consisting of thick peptidoglycan) is more vulnerable to the effects of GO and showed better antibacterial rate [94]. In the case of Total alkaloids from Semen Strychnine (TASS), an antibacterial drug, loaded PEEK/ polyglycolide acid composite, *E. coli* gave superior results compared to *S. aureus* due to its thinner cytoderm that enabled TASS infiltration. The cell membrane thickness of *E. coli* was about 10 nm, whereas this value varied between 20 and 80 nm for *S. aureus* [144]. Tantallum-included systems gave moderate to low antibacterial rates in the studies reviewed [115, 149]. Therefore, a combination with genistein improved the antibacterial rate [115]. The mechanism was explained by the electrostatic interaction between negative charges of the bacterial cell membrane and positive charges of the tantallum ions on the surface. The interaction caused cell wall leakage and bacterial cell death [115].

**Table 5.** The antibacterial effect of the modification with reinforcements.

| | Reinforcement | Production method | High (Bacterial effect > 80%) | Moderate (Bacterial effect between 80%–50%) | Low (Bacterial effect < 50%) | Reference |
|---|---|---|---|---|---|---|
| Drugs, Peptides, Proteins and Polymers | TASS (7.5 wt. %) and PGA[a] | Selective Laser Sintering | | *E. coli* | *S. aureus* | [144] |
| | Lactam (0.931 mg $g^{-1}$) | Solution mixing with sulfonated PEEK | *S. mutans* (In biofilm form) | | | [90] |
| Ions, Functional groups, Nanoparticles | $TiO_2$ (16 wt. %) | Injection molding | | | *E. coli, B. subtilis* | [51] |
| | $SiO_2$ (12 wt. %) | Injection molding | | | *E. coli, B. subtilis* | [51] |
| | $TiO_2$ (8 wt. %), $SiO_2$ (8 wt. %) | Injection molding | *E. coli* | *B. subtilis* | | [51] |
| | Nano-ZnO (7.5 wt. %) | Hydrothermal growth, melt blending and injection molding | | | *E. coli, S. aureus* | [63] |
| | ZnO (7.5 wt. %) modified with silane coupling agent (APTMS[b]) | Cryogenic ball-milling and compression moulding | *E. coli, S. aureus* | | | [154] |
| | Nanofluorohydroxyapatite (5 wt. %) | Powder blending and compression molding | *S. mutans* | | | [91] |
| | α-$S_3N_4$ (15 vol. %) | Twin-screw extrusion | *S. epidermidis* | | | [54] |
| | β-$S_3N_4$ (15 vol. %) | Twin-screw extrusion | | *S. epidermidis* | | [54] |
| | β-SiYAlON[c] (15 vol. %) | Twin-screw extrusion | | | *S. epidermidis* | [54] |
| | Black Phosphorus (0.5 wt. %) | Powder mixing with PEEK/PTFE[d] (10 wt. %) in ethanol and compression molding | *S. aureus* | | | [92] |
| | Nano-Tantalum (50% v/v) | Cold pressing sintering | | *S. aureus* | *E. coli* | [149] |
| | Nano-Silicon nitride(50% v/v) | Cold pressing sintering | *E. coli, S. aureus* | | | [149] |
| | Nano-Ag-$TiO_2$ (4 wt. %) | Powder mixing and compression molding | *S. aureus* | | | [155] |
| | Tantalum pentoxide (50% v/v) | Cold pressing and sintering | | | *E. coli, S. aureus* | [115] |
| | GO (0.02 wt. %)/Carbon fibers (25 wt. %) | Twin-screw extrusion and grinding | *S. aureus, S. mutans* | | *E. coli* | [94] |

(Continued.)

**Table 5.** (Continued.)

| | Reinforcement | Production method | High (Bacterial effect > 80%) | Moderate (Bacterial effect between 80%–50%) | Low (Bacterial effect < 50%) | Reference |
|---|---|---|---|---|---|---|
| Combination of polymers, drugs and nanoparticles | *n*-$TiO_2$ (5 wt. %) and PGAa HA (3 g $l^{-1}$) and Chitosan (0.05 g) | Selective Laser Sintering | *E. coli, S. aureus* | | | [79] |
| | | Solution mixing with PEEK (20%) and elecrophoretic deposion | *E. coli, S. aureus* | | | [83] |

[a] PGA: Polyglycolic acid (for improvement biocompatibility and biodegradability).

[b] 3-Aminopropyl)trimethoxysilane.

[c] β-SiYAlON: A compound consists of $Si_3N_4$, $Al_2O_3$, and $Y_2O_3$, blended and reacted in $N_2$ gas atmosphere at >1600 °C for 2 h. The atomic ratios; N/Si:1.02, O/Si: 0.5, and Y/Si:0.064.

[d] Polytetrafluoroethylene.

The mechanical properties are not altered by changing the surface properties. The composite production method enables tailoring the mechanical properties of PEEK. PEEK polymer has an elastic modulus (3–4 GPa), which can be tailored to have close values with cortical bone (18 GPa) [8]. The implant's elastic modulus that matches the bone results in reduction in stress shielding. A study analyzed stress distribution at the implant and bone interface using 3D-FEM. This property is important in terms of the initial stability of the implant and directly affects the success of the implant. The composition with 8 wt.% $TiO_2$, 8 wt.% $SiO_2$ and 84 wt.% PEEK gave the minimum stress distribution with trapezium profile thread [51].

Wear is another problem that causes implant failure by loosening or debris formation. Wear resistance and friction coefficient are essential parameters for artificial joint composites. ZnO nanoparticles were incorporated to obtain a wear-resistant PEEK implant material. When the addition amount was 5 wt.%, the wear rate decreased by 68% compared to PEEK polymer [63]. Black phosphorus is another reinforcement used in PEEK composite to improve the wear properties. The wear rate decreased 95% when 10 wt.% PTFE and 0.5 wt.% black phosphorus were included in the PEEK structure [92]. Black phosphorus formed a transfer film with Van der Waals force, providing a good adhesion with tribopairs [92]. PEEK composite coatings with carbon fiber (25 wt.%) and GO (0.02 wt.%) improved the wear resistance of Ti–6Al–4V alloy [94]. The composites of PEEK/ nano-ZnO (7.5 wt.%) and short carbon fiber (15 wt%) showed better wear performance and lower friction coefficient compared to the pristine PEEK [150].

Antibacterial and osteogenic properties were also investigated concurrently in most of the studies. The observations based on fluorescence staining showed that the morphology of mouse chondroblasts ADTC5 cells had a flat strip shape on day seven, which was the indicator of proliferation and differentiation [63]. Similarly, nano$TiO_2$ (addition amounts: 1, 3, 5, and 7 wt.%) enhanced the proliferation and attachment of MG-63 cells when it is used as a reinforcement in PEEK/PGA blend [79]. 40 wt.% addition of nano-fluorohydroxyapatite into PEEK improved alkaline phosphatase activity and biomineralization activity of MG-63 cells (human osteoblast-like cells) [91]. Silicon nitride/PEEK (v/v 50%) and Tantalum/PEEK (v/v 50%) enhanced MC3T3-E1 cell proliferation and differentiation *in vitro* and new bone formation and osseointegration *in vivo* [149].

The systems with antibiotics are effective in planktonic bacteria. However, when the bacteria become colonized and form biofilms, the concentration of antibiotics used in the treatments should be increased a thousand times [90]. Therefore, the antibiofilm efficacy is an important property for an implant material. In a PEEK/lactam composite coating study, the prevention of biofilm formation is provided by lactam addition after surface functionalization with sulfonation [90]. Similarly, the biofilm formation deteriorated by 40 wt.% nano-fluorohydroxyapatite addition into PEEK. There were lots of dead *S. mutans* bacteria detected on the samples compared to pristine PEEK after adding 40 wt.% nano-fluorohydroxyapatite. Fluoride ions inhibit bacterial metabolism and dental plaque acidogenicity [91].

In the case of nano-ZnO, a gradual increase in antibacterial properties with nano-ZnO addition was seen [63, 154]. The maximum antibacterial property was reached at 7.5 wt. % [154]. Modifying ZnO nanoparticles with a silane coupling agent, APTMS, prevented the release of ZnO nanoparticles. The increasing trend of the antibacterial property with ZnO content was explained by ROS ($H_2O_2$) generation [154]. The different responses of *E. coli* and *S. aureus* against $H_2O_2$ supported the experimental results since *E. coli*

is affected more by ZnO content [154]. The effect of short carbon fiber in the ZnO/PEEK composite structure was investigated. The 15 wt. % addition of short carbon fiber increased the zone of inhibition from 11.95 mm to 28.9 mm for *E. coli* and 11.43–22.2 mm for *S. aureus* [150].

The gradual increase of antibacterial effect for *n*-$TiO_2$ was up to 5 wt. % [79]. Adding *n*-$TiO_2$ higher than 5 wt. % reduced the effective surface-to-volume ratio due to the formation of clusters. Therefore, the interaction between the material and bacteria decreased [79]. Another reinforcement, $S_3N_4$, affected the antibacterial property of PEEK. The reaction between the aqueous environment and $S_3N_4$ released ammonia and silicic acid from the surface of $S_3N_4$. Ammonia increased the extracellular pH and triggered the formation of free radicals, resulting in death in some bacteria [54].

Similarly, another silicon-based compound, silicon nitride included $–NH_2$ groups and gave $–NH_3^+$ ions to the environment. The negatively charged bacterial cell wall interacted with positively charged ions and destructed. Moreover, the alkaline environment formed by $–NH_3^+$ ions affected biofilm formation negatively [149].

Besides ceramics, an organic compound, gelatin was used as a reinforcement. Gelatin killing counts were 32.6% and 39.2% against *S. aureus* and *E. coli*, respectively. It was shown that PEEK/gelatin nanocomposites studied in hydrogel form increased bacteria killing counts from 23.3% (for pure PEEK) to 57.1% against *S. aureus* and 34.7% (for pure PEEK) to 61.8% against *E. coli*. The PEEK/gelatin weight ratio was 1.73 to obtain the hydrogel [64].

### 4.4. Changing the surface topography

Surface topography is a property that defines surface adhesion. The surface features smaller than the bacterial size inhibit the bacterial attachment [156–160]. The methods for the surface texture of PEEK for better antibacterial efficiency are cold plasma treatment, sulfonation, plasma immersion ion implantation, and micro/nano array formation by colloidal lithography, plasma etching, forming laser-induced periodic surface structures (figure 5). Table 6 summarizes the treatments to change surface topography to improve the antibacterial property of PEEK. Changing the surface topography is the least studied, and relatively less effective results were obtained regarding antibacterial properties. The plasma immersion ion implantation method is widely used to change the surface topography. This method gave relatively high antibacterial results for the Zn and O ions combination and $TiO_2$ ions [161, 162]. On the other hand, cold plasma technique with Ar improved the antibacterial property below 20%, and the reduction was improved with the contribution of $N_2$ [60].

Colloidal lithography and plasma etching have produced cones and pillars in nano and micro dimensions. The antibacterial tests on *E. coli* showed that the dimensions and density of microstructures gave more effective results than nanostructures. Moreover, the cone shape increased the antibacterial rate compared to the pillar shape due to its sharp edges [168]. In another study, the KrF excimer laser was used to obtain ∼100 nm wide stripes on the PEEK surface. Moreover, the structure was decorated with Ag nanoparticles. The surface structured samples showed better antibacterial properties, although they had lower Ag concentration than the untreated samples [169].

As seen in table 6, zinc and oxygen plasma immersion ion implantation on carbon fiber reinforced PEEK gave the highest antibacterial results on *MRSA, S. aureus* and *S. epidermidis* in 24 h compared to plasma immersion ion implantation of $N_2$ [161, 167]. The trap-killing mechanism of the surface topography by forming micro pits with dimensions (∼800 nm) that fit the bacteria showed a reduction higher than 90% in *MRSA, S. aureus* and *S. epidermidi.* In contrast, no antibacterial effect was seen on *E. coli* and *P. aeruginosa* [161]. In the case of $TiO_2$ plasma immersion ion implantation, nanoparticles with the dimension of about 20 nm prevent bacterial adhesion of *S. mutans, F. nucleatum* and *P. gingivalis* by providing less attachment area [162]. Moreover, antibacterial longevity was tested for 28 d and above 80% of antibacterial rates were obtained. Similarly, the significant difference between the antibacterial rates of *S. aureus* (71.4%) and *E. coli* (5.3%) stemmed from their different shapes. *E. coli* has an elongated shape that reduces the direct contact with the surface of PEEK treated with $TiO_2$ plasma immersion ion implantation and decreases the effect of ROS [166].

PEEK polymer is classified as bioinert; therefore, in most of the applications, osseointegration is limited. Since its high chemical resistance, the modification techniques gain importance in studies of PEEK as an implanted biomaterial. Similar techniques to increase antibacterial properties are applied to increase biocompatibility of PEEK. Cold plasma technique with argon and $N_2$, was shown *in vitro* to increase the biocompatibility [60]. The best results for osteogenic activity were obtained for the $N_2$ treated samples. Therefore, those samples showed an efficient race-for-the-surface property. Similarly, the nitric and sulfric acid mixture increased bioactivity and cell biocompatibility [84]. When the surface was treated with argon plasma immersion ion implantation and hydrofluoric acid, rat bone mesenchymal stem cell adhesion, spreading, proliferation and ALP activity enhanced on the fluorinated surface of PEEK [107].

#### *4.4.1. Cold plasma technique*

Cold plasma is a nonthermal technique that uses partially ionized positive and negative ions, free radicals, gas-containing molecules, and charged particles

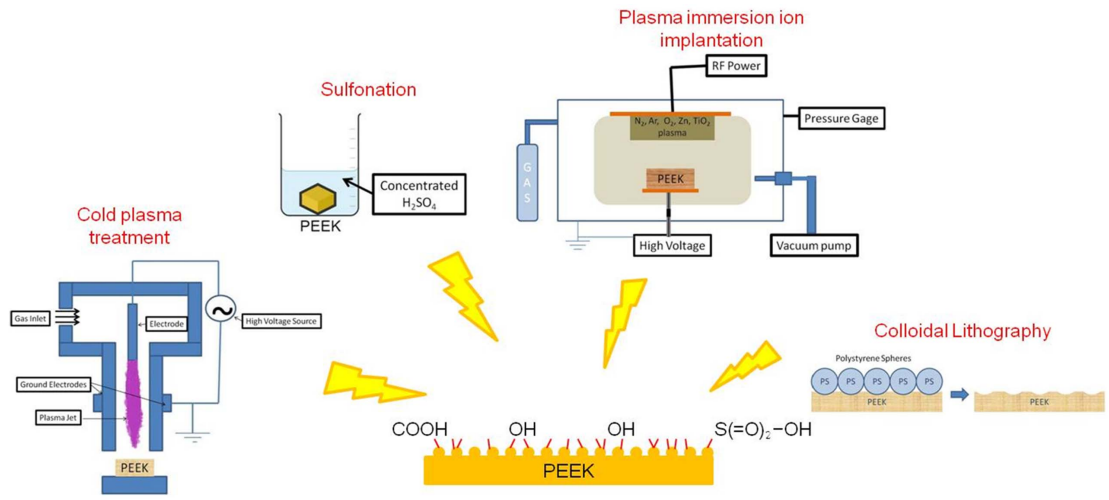


**Figure 5.** The methods for changing PEEK's surface and addition of functional groups. The methods widely used are sulfonation, cold plasma treatment, and plasma immersion ion implantation. Sulfonation, other acid treatmets, and plasma immersion ion implantation methods change the surface topography and incorporate ions such as $SO_3H$, $NO_2$, $Zn^{2+}$, and $O^{2-}$ to the surface [84, 99, 161]. The cold plasma technique changed the surface roughness and dendritic or scaly nanoprotrusions were obtained on the surface [60]. The figures that represent cold plasma treatment [163] and plasma immersion ion implantation [164] figures are adapted with permission. Colloidal lithography figure is reprinted (adapted) with permission from [165]. Copyright 2017 American Chemical Society [163]. [05/07/2022], adapted with permission of the publisher (Taylor & Francis Ltd, www.tandfonline.com.) Adapted from [164]. CC BY 4.0. Reprinted with permission from [165]. Copyright (2017) American Chemical Society.

**Table 6.** The antibacterial effect of the modification with changing the surface topography.

| Modification methodr | High(Bacterialeffect > 80%) | Moderate(Bacterialeffect between 80-50%) | Low(Bacterial effect<50%) | Reference |
|---|---|---|---|---|
| Cold plasma with Ar | | | *S. mutans, S. aureus* | [60] |
| Cold plasma with Ar (90%) and $N_2$ (10%) | | | *S. mutans, S. aureus* | [60] |
| Plasma immersion ion implantation (Nanostructured $TiO_2$) | *F. Nucleatum* | *S. mutans, P. gingivalis, S. aureus* | *E. coli* | [162, 166] |
| Mixing with $HNO_3$ (conc:65%) and $H_2SO_4$ (conc:98%) (1:1) and refluxing with ethylenediamine | | *S. aureus, E. coli* | | [84] |
| Zinc and oxygen plasma immersion ion implantation on carbon fiber reinforced PEEK | *S. aureus, S. epidemidis, MRSA* | | *E. coli, P. aeruginosa* | [161] |
| Nitrogen plasma immersion ion implantation | | | *S. aureus* | [167] |
| Argon plasma immersion ion implantation | | *P. gingivalis* | | [107] |
| Colloidal lithography and plasma etching of polystyrene spheres | *E. coli* (Nanocones) | *E. coli* (Nanopillars) | | [168] |

in the form of electrons and protons. The method is used for bonding, curing polymers, and increasing antibacterial effectiveness [170].

Changing the gas composition in the cold plasma technique resulted in different topographic structures. For example, 25 min of treatment with Ar showed regularly arranged scaly nanoprotrusions, whereas $N_2$ formed dendritic nanoprotrusions. When the gas composition was arranged as 90% Ar/10% $N_2$, an unorganized and scaly texture with the densest and finest nanoprotrusions was observed according to the SEM results [60]. Therefore, the highest antibacterial rate was seen for the samples treated with a gas content of 90% Ar/10% $N_2$. The area for bacterial adhesion and the interaction between bacteria and the surface decreased. The morphology of *S. aureus* was observed with SEM on cold plasma-treated PEEK samples [60]. Bacteria have a spherical shape on untreated samples with a smooth and continuous cell membrane.

On the other hand, in the samples treated with 90% Ar/10% $N_2$, the bacteria chain length was shorter, and destructed cell membranes were observed. Pre-annealing (10 °C $min^{-1}$–180 °C) changed the types of nanolamellae formed by argon plasma treatment for 45 min [171]. Verticle and tilted nano lamellae increased antibacterial efficiency against *S. aureus* and *E. coli*, significantly compared to PEEK samples treated with argon plasma treatment for 5 min [171]. Without annealing, verticle nano lamellae were obtained. Verticle nano lamellae were more destructive against *S. aureus* and *E. coli* than tilted nano lamellae that were produced with pre-annealing [171].

Moreover, roughness and breakage in the cell membrane were observed, indicating better antibacterial properties than untreated samples [60]. Similarly, SEM and live/dead staining images showed that *E. coli* and *S. aureus* had irregular shapes due to bacterial lysis and distortion of the membranes after Ar-plasma treatment of sulfonated PEEK for 5 and 10 min [46]. Since plasma treatment formed nanoprotrusions on the surface, *E. coli* (1 μm) and *S. aureus* (0.5 μm) contact area decreased. Therefore, the adhesion of bacteria was inhibited [46]. An electrostatic repulsion between the surface and the bacteria was formed by Ar-plasma treatment, adding carboxyl, hydroxyl, and sulfonic acid groups on the surface, increasing electronegativity [46].

#### *4.4.2. Plasma immersion ion implantation*

Plasma immersion ion implantation is a technique for changing the surface topography of semiconductors, metals and dielectrics [172]. In this technique, the target is surrounded by the plasma; therefore, the method can be used for 3D geometries [173]. The flux of energetic plasma ions is implanted on the surface using high negative voltages [172]. $TiO_2$, $Zn^{2+}$, and $O^{2-}$ ions and $N_2$ are molecules used to obtain a surface texture on PEEK with antibacterial properties by using this technique.

$TiO_2$ nanopores with 150–200 nm diameters were obtained by plasma immersion ion implantation on carbon fibers and PEEK composites [162]. Since there was no release of Ti ions from the structure, the antibacterial improvement was attributed to the surface structure containing 20 nm nanoparticles [162, 166]. The small dimension of the nanoparticles decreased the contact area between the substrate and bacteria and inhibited bacterial adhesion. Moreover, according to x-ray photoelectron spectroscopy results, possible vacancies of oxygens in the nanostructure increased with the depth of $TiO_2$ [162]. Oxygen vacancies in $TiO_2$ were highly reactive and produced ROS, damaging bacteria [162].

Zinc and oxygen ions were implemented on carbon fiber-reinforced PEEK using the plasma immersion ion implantation method [161]. According to the antibacterial studies, there was no significant change in antibacterial efficiency with a low amount of Zn ion release. The results showed that the topography, which formed micro-pits with a diameter of about 800 nm, impacted the antibacterial properties of *S. aureus, MRSA*, and *S. epidemidis* [161]. The bacteria with the similar size micro-pits (800 nm) were trapped in the pits and could not provide interconnectivity with the bacterium. Therefore, biofilm formation was inhibited [161]. $N_2$-treated samples with the same method showed a 19% reduction in bacterial growth [167]. The surface roughness of the treated samples was lower than 900 nm which was within the limit for bacterial attachment (between 10 nm and 900 nm) [167]. Therefore, the effect of $N_2$-containing functional groups on bacterial activity was hypothesized [167].

## 5. Conclusion and prospect

According to the studies aimed at designing new biomaterials with antibacterial properties for infection control in dental and orthopedic surgery applications, immobilization of an antibacterial agent provides a more controllable environment in which the release profile of the immobilized compounds can be adjusted easily without changing the dimensions of the implant. For example, 6 months should be covered for better attachment to avoid early-stage dental implant failure. Moreover, immobilization eliminates the cracks and bulky release of the antibacterial material compared to the coatings. Another critical issue is the timing of the osteoblast attachment and bacterial attachment. The race-for-the-surface between the osteoblasts and bacteria defines the success of the implant. Therefore, antibacterial agents possessing longevity in release and functional compounds enhancing osteoblast attachment

are required. Dual systems formed by immobilizing an antibacterial agent and compounds with osteogenic origin promote osteoblast attachment and inhibit bacteria simultaneously. Therefore, those systems are superior to PEEK nanocomposites and coated PEEK in the scope of antibacterial effects. Forming nanocomposites, coating, and changing surface topography can enhance the immobilization of functional materials and support them in antibacterial ability.

The limitations of PEEK used in dental applications as endo-crowns and abutments are loosening and infection [18]. Modifications to prevent loosening and infection are listed as sustained release of antibacterial material, a composition showing high osseointegration, and elastic modulus values close to bone located in reconstruction areas. Regarding orthopedic implants, PEEK is used as cranioplasty and maxillofacial reconstruction implants, fixation devices, spinal implants and joint replacements (knee and hip) [18]. In spinal implants, poor osseointegration is detected as a main problem. Loosening and infection are common for the cranioplasty and maxillofacial reconstruction implants, fixation devices, and joint replacements [18].

Mechanical properties can be altered by only producing composites, whereas osseointegration and antibacterial properties can be enhanced by coating, immobilizing molecules on the surface, and changing the surface texture. The elastic modulus can be increased using reinforcements such as $TiO_2$ and $SiO_2$ to provide better osseointegration [51]. Moreover, sustained release should be provided to support osteoblasts for race-for-the surface for the coating application with a start of a burst release. A sudden drug release between five to seven days should be provided to prevent biofilm formation. Since most of the studies were conducted at pH 7.4, the compounds that are effective in several pH values should be used according to the application area, especially for dental applications, because of sudden changes in pH of the oral environment. Therefore, a layer-by-layer approach would be an good solution to control the release amount and time [51, 117]. It is possible to construct a system that provides a burst release of an antibacterial agent at the first layer and a sustained release of an antibacterial agent combination with a compound that supports osseointegration. $Ag^+$ ion gave inhibition rates of bacteria higher than 90% in all types of applications [3, 52, 117]. Therefore, a compound including $Ag^+$ ion would be a good choice as a burst release layer. However, cytotoxicity should be considered because initial burst of $Ag^+$ inhibited MC3T3-E1 cells in the first 3 d [97]. The high porosity of the carrier and weak bonds between the antibacterial agent and carrier resulted in a high initial burst [75].

Phototermal therapy is another approach to regulating antibacterial properties. A sudden increase in the temperature at the infection site can be provided using the photothermal ability of coated materials instead of the burst release of an antibacterial agent [120, 135].

The spectrum of the antibacterial agent is another parameter that should be considered. An antibacterial agent with a broad spectrum is required for dental applications since the oral environment contains several types of bacteria that result in oral diseases [174]. As a testing model, bacteria representing the initial (*S. sanguini)* and late (*P.gingivalis*) colonization periods should be chosen [68]. On the other hand *S. marcescens* becomes prominent for the spinal infections [136]. Therefore, drugs with broad spectrum should be chosen for more efficient antibacterial therapy. The amount of antibacterial agent is also a parameter to regulate the antibacterial properties. The reduction in concentration decreased the release amount [48].

The bioinertness and chemically inertness of PEEK are the challenges researchers face during their studies. Surface modification techniques such as sulfonation and coating with PDA were used in most of the studies to overcome chemical inertness of PEEK. The proposed systems should support antibacterial and osteogenic properties to overcome the bioinertness. The antibacterial agent's type and its concentration optimization are crucial parameters. For example, although Ag is a superior antibacterial agent, it causes cytotoxicity. Therefore, the amount of Ag should be optimized. The most used modification techniques to obtain the antibacterial property are immobilizing an antibacterial agent and coating PEEK with an antibacterial material. Those modifications are obtained by immersion and dip coating. Although those methods are easy to apply and cost-effective, non-homogenous surfaces can be obtained which resulted in failed results. Another problem is to find a broad spectrum antibacterial material. As seen in most of the studies, the response of bacteria changes based on the antibacterial agent.

Smart biomaterials are another area that emerged in the field [175]. Since there were some examples of photo-responsive [57, 120, 135] and pH-responsive [137, 138] systems for PEEK, other techniques such as enzyme-responsive, electrical stimuli-responsive, vibration-responsive and magnetic-responsive systems can be developped for PEEK implants to provide a solution-oriented approach and better control over drug release, biocompatibility and antibacterial efficiency [175]. Salivary and bacterial enzymes can be used as a stimulus for releasing antibacterial agents. The charges on the biofilms are the starting point of the electrical-stimuli responsive materials. The combination with $Fe_3O_4$ adds a magnetic responsiveness to the material. $BaTiO_3$ gives a piezoelectric property to the material affects biofilms when there is only mechanical stimulation [176].

A successful biomaterial for implants should provide the best osseointegration to avoid implant

rejection and revision. Although PEEK has an advantage in its mechanical properties, it is a bioinert material and requires modifications to render antibacterial and osseointegration properties. Being a chemically inert biomaterial, PEEK challenges the researchers in the field in modification techniques. The most widely used techniques to overcome PEEK's chemical inertness are sulfonation and PDA coating. Bioactive molecules/compounds are attached to the surface of PEEK with the help of those techniques to bring antibacterial and biocompatibility properties to this material.

This review summarizes the strategies to improve PEEK's antibacterial properties. Moreover, the measurement methods and the mechanisms of bacterial inhibition are explained. According to the studies analyzed, the immobilization of functional groups and compounds has been studied the most. It was reasonable since immobilizing the functional groups provided a more controllable release profile for antibacterial purposes. Moreover, the osteogenic properties of the PEEK can be tailored by adding different functional groups. $Ag^{+}$ ions, Ag nanoparticles, and various antibiotics for immobilization are mainly used agents. Bone-forming and osteogenic growth peptides have been used to add osteogenic properties to the system. The coating materials included Ag, Cu, Zn, and Mg elements, ceramics (HA, brushite), drugs (cefuroxime sodium salt, tobramycin, and GS), red/gray selenium nanorods, and black/white tantalic oxides. Immersion and dripping are the two most used methods for coating and immobilizing functional groups. The blending method is used widely to form PEEK composites with $TiO_2$, $SiO_2$, ZnO, HA, lactam, black phosphorus, and $S_3N_4$ to add an antibacterial effect. Cold plasma technique, plasma immersion ion implantation, and treatment with a strong acid are methods used to change the surface topography to enhance the antibacterial properties of PEEK. ROS generation is the main mechanism for the antibacterial effect, and colony-forming unit calculation is used widely as a quantitative measurement method to detect antibacterial properties.

## Data availability statement

All data that support the findings of this study are included within the article (and any supplementary files).

## Funding

This research did not receive any specific Grant from funding agencies in the public, commercial, or not-for-profit sectors.

## ORCID iDs

Idil Uysal https://orcid.org/0000-0002-9687-8787
Ayşen Tezcaner https://orcid.org/0000-0003-4292-5856
Zafer Evis https://orcid.org/0000-0002-7518-8162

## References

[1] Campoccia D, Montanaro L and Arciola C R 2006 The significance of infection related to orthopedic devices and issues of antibiotic resistance *Biomaterials* **27** 2331–9
[2] Bollen C M L, Papaioanno W, Van Eldere J, Schepers E, Quirynen M and Van Steenberghe D 1996 The influence of abutment surface roughness on plaque accumulation and peri-implant mucositis *Clin. Oral Implants Res.* **7** 201–11
[3] Liu X, Gan K, Liu H, Song X, Chen T and Liu C 2017 Antibacterial properties of nano-silver coated PEEK prepared through magnetron sputtering *Dent. Mater.* **33** e348–60
[4] Soutis C 2005 Carbon fiber reinforced plastics in aircraft construction *Mater. Sci. Eng.* A **412** 171–6
[5] Tusavul S, Fragoudakis R, Saigal A and Zimmerman M A 2014 Thermoplastic materials for wind turbine blade design *The 2014 World Congress on Advances in Civil, Environmental, and Materials Research (ACEM14)* (*Busan*)
[6] May R 2008 Polyethertherketones *Encyclopedia of Polymer Science and Technology* vol 12 (ICI Americas, Inc.) pp 313–20
[7] Liao K 1994 Performance characterization and modeling of a composite hip prosthesis *Exp. Tech.* **18** 33–38
[8] Kurtz S M and Devine J N 2007 PEEK biomaterials in trauma, orthopedic, and spinal implants *Biomaterials* **28** 4845–69
[9] Mavrogenis A F, Vottis C, Triantafyllopoulos G, Papagelopoulos P J and Pneumaticos S G 2014 PEEK rod systems for the spine *Eur. J. Orthop. Surg. Traumatol.* **24** 111–6
[10] Roziére J and Jones D J 2003 Non-fluorinated polymer materials for proton exchange membrane fuel cells *Annu. Rev. Mater. Res.* **33** 503–55
[11] Kerres J A 2001 Development of ionomer membranes for fuel cells *J. Membr. Sci.* **185** 3–27
[12] Green S and Schlegel J 2001 A polyaryletherketone biomaterial for use in medical implant applications *Polym. Med. Ind. Proc. Conf. Held Brussels* pp 1–7
[13] Brown S A, Hastings R S, Mason J J and Moet A 1990 Characterization of short-fibre reinforced thermoplastics for fracture fixation devices *Biomaterials* **11** 541–7
[14] Chacón-Moya E, Gallegos-Hernández J F, Piña-Cabrales S, Cohn-Zurita F and Goné-Fernández A 2009 Cranial vault reconstruction using computer-designed polyetheretherketone (PEEK) implant: case report *Cir Cir* **77** 437–40
[15] Foletti J M, Lari N, Dumas P, Compes P and Guyot L 2012 Reconstruction esthétique de la voûte crânienne par implant sur mesure en PEEK *Rev. Stomatol. Chir. Maxillofac.* **113** 468–71
[16] Wang A, Lin R, Stark C and Dumbleton J H 1999 Suitability and limitations of carbon fiber reinforced PEEK composites as bearing surfaces for total joint replacements *Wear* **225–229** 724–7
[17] Skinner H B 1988 Composite technology for total hip arthroplasty *Clin. Orthop. Relat. Res.* **235** 224–36
[18] He M, Huang Y, Xu H, Feng G, Liu L, Li Y, Sun D and Zhang L 2021 Modification of polyetheretherketone

implants: from enhancing bone integration to enabling multi-modal therapeutics *Acta Biomater.* **129** 18–32
[19] Ma T, Zhang J, Sun S, Meng W, Zhang Y and Wu J 2023 Current treatment methods to improve the bioactivity and bonding strength of PEEK for dental ap plication: a systematic review *Eur. Polym. J.* **183** 111757
[20] Verma S, Sharma N, Kango S and Sharma S 2021 Developments of PEEK (Polyetheretherketone) as a biomedical material: a focused review *Eur. Polym. J.* **147** 110295
[21] Zhou J, Xia Q, Dong J, Li X, Zhou X, Fang T and Lin H 2011 Comparison of stand-alone polyetheretherketone cages and iliac crest autografts for the treatment of cervical degenerative disc diseases *Acta Neurochir.* **153** 115–22
[22] Thien A, King N K K, Ang B T, Wang E and Ng I 2015 Comparison of polyetheretherketone and titanium cranioplasty after decompressive craniectomy *World Neurosurg.* **83** 176–80
[23] Kim M M, Boahene K D O and Byrne P J 2009 Use of customized polyetheretherketone (PEEK) implants in the reconstruction of complex maxillofacial defects *Arch. Facial Plast. Surg.* **11** 53–57
[24] Jia Z, Xu X, Zhu D and Zheng Y 2023 Design, printing, and engineering of regenerative biomaterials for personalized bone healthcare *Prog. Mater. Sci.* **134** 101072
[25] Kang J, Zhang J, Zheng J, Wang L, Li D and Liu S 2021 3D-printed PEEK implant for mandibular defects repair—a new method *J. Mech. Behav. Biomed. Mater.* **116** 104335
[26] Haleem A and Javaid M 2019 Polyether ether ketone (PEEK) and its manufacturing of customised 3D printed dentistry parts using additive manufacturing *Clin. Epidemiol. Glob. Health* **7** 654–60
[27] Mirkhalaf M, Men Y, Wang R, No Y and Zreiqat H 2023 Personalized 3D printed bone scaffolds: a review *Acta Biomater.* **156** 110–24
[28] Pulipaka A, Gide K M, Beheshti A and Bagheri Z S 2023 Effect of 3D printing process parameters on surface and mechanical properties of FFF-printed PEEK *J. Manuf. Process.* **85** 368–86
[29] Francis J N, Banerjee I, Chugh A and Singh J 2022 Additive manufacturing of polyetheretherketone and its composites: a review *Polym. Compos.* **43** 5802–19
[30] Zheng J *et al* 2022 Additively-manufactured PEEK/HA porous scaffolds with excellent osteogenesis for bone tissue repairing *Composites* B **232** 109508
[31] Zhang C, Wang L, Kang J, Fuentes O M and Li D 2020 Bionic design and verification of 3D printed PEEK costal cartilage prosthesis *J. Mech. Behav. Biomed. Mater.* **103** 103561
[32] Gorth D J, Puckett S, Ercan B, Webster T J, Rahaman M and Sonny Bal B 2012 Decreased bacteria activity on $Si_3N_4$ surfaces compared with PEEK or titanium *Int. J. Nanomed.* **7** 4829–40
[33] Bächle J, Merle C, Hahnel S and Rosentritt M 2023 Bacterial adhesion on dental polymers as a function of manufacturing techniques *Materials* **16** 2373
[34] Ma Z, Zhao X, Zhao J, Zhao Z, Wang Q and Zhang C 2020 Biologically modified polyether ether ketone as dental implant material *Front. Bioeng. Biotechnol.* **8** 1–17
[35] Chen J, Cao G, Li L, Cai Q, Dunne N and Li X 2022 Modification of polyether ether ketone for the repairing of bone defects *Biomed. Mater.* **17** 042001
[36] Gao W, Han X, Li Y, Zhou Z, Wang J, Shi R, Jiao J, Qi Y, Zhou Y and Zhao J 2022 Modification strategies for improving antibacterial properties of polyetheretherketone *J. Appl. Polym. Sci.* **139** 1–12
[37] Pidhatika B, Widyaya V T, Nalam P C, Swasono Y A and Ardhani R 2022 Surface modifications of high-performance polymer polyetheretherketone (PEEK) to improve its biological performance in dentistry *Polymers* **14** 1–38
[38] Kligman S, Ren Z, Chung C-H, Perillo M A, Chang Y-C, Koo H, Zheng Z and Li C 2021 The impact of dental implant surface modifications on osseointegration and biofilm formation *J. Clin. Med.* **10** 1641
[39] Wang Y, Zhang S, Nie B, Qu X and Yue B 2022 Approaches to biofunctionalize polyetheretherketone for antibacterial: a review *Front. Bioeng. Biotechnol.* **10** 1–15
[40] Liu Y, Fang M, Zhao R, Liu H, Li K, Tian M, Niu L, Xie R and Bai S 2022 Clinical applications of polyetheretherketone in removable dental prostheses: accuracy, characteristics, and performance *Polymers* **14** 4615
[41] Toumeh T, Sghaireen M, Ganji K, Mathew M, Nagy A and Rao K 2020 A review on biofilm and biomaterials: prosthodontics and periodontics perspective *J. Int. Oral Health* **12** 504–11
[42] Brum R S, Labes L G, Volpato C Â M, Benfatti C A M and Pimenta A D L 2020 Strategies to reduce biofilm formation in peek materials applied to implant dentistry—a comprehensive review *Antibiotics* **9** 1–21
[43] Wei Z, Zhang Z, Zhu W and Weng X 2023 Polyetheretherketone development in bone tissue engineering and orthopedic surgery *Front. Bioeng. Biotechnol.* **11** 1–16
[44] Kratochvíl J, Štěrba J, Lieskovská J, Langhansová H, Kuzminova A, Khalakhan I, Kylián O and Straňák V 2018 Antibacterial effect of Cu/C:F nanocomposites deposited on PEEK substrates *Mater. Lett.* **230** 96–99
[45] Pang G, Yi M, Yin X, Wu W and Xu S 2022 Immobilization of chitosan on polyether ether ketone surface modified with acrylic acid by UV-induced graft polymerization *Iran. Polym. J.* **31** 1399–407
[46] Wang S, Deng Y, Yang L, Shi X, Yang W and Chen Z G 2018 Enhanced antibacterial property and osteo-differentiation activity on plasma treated porous polyetheretherketone with hierarchical micro/nano-topography *J. Biomater. Sci. Polym. Ed.* **29** 520–42
[47] Xu X *et al* 2019 Triple-functional polyetheretherketone surface with enhanced bacteriostasis and anti-inflammatory and osseointegrative properties for implant application *Biomaterials* **212** 98–114
[48] Tran N, Kelley M N, Tran P A, Garcia D R, Jarrell J D, Hayda R A and Born C T 2015 Silver doped titanium oxide-PDMS hybrid coating inhibits Staphylococcus aureus and Staphylococcus epidermidis growth on PEEK *Mater. Sci. Eng.* C **49** 201–9
[49] Berlanga M and Guerrero R 2016 Living together in biofilms: the microbial cell factory and its biotechnological implications *Microb. Cell Factories* **15** 1–11
[50] Gao C, Wang Z, Jiao Z, Wu Z, Guo M, Wang Y, Liu J and Zhang P 2021 Enhancing antibacterial capability and osseointegration of polyetheretherketone (PEEK) implants by dual-functional surface modification *Mater. Des.* **205** 109733
[51] Muthusamy Subramanian A V and Thanigachalam M 2022 Mechanical performances, *in-vitro* antibacterial study and bone stress prediction of ceramic particulates filled polyether ether ketone nanocomposites for medical applications *J. Polym. Res.* **29** 318
[52] Yan J, Zhou W, Jia Z, Xiong P, Li Y, Wang P, Li Q, Cheng Y and Zheng Y 2018 Endowing polyetheretherketone with synergistic bactericidal effects and improved osteogenic ability *Acta Biomater.* **79** 216–29
[53] Wang Q, Mejía Jaramillo A, Pavon J J and Webster T J 2016 Red selenium nanoparticles and gray selenium nanorods as antibacterial coatings for PEEK medical devices *J. Biomed. Mater. Res.* B **104** 1352–8
[54] Pezzotti G *et al* 2018 Incorporating $Si_3N_4$ into PEEK to produce antibacterial, osteocondutive, and radiolucent spinal implants *Macromol. Biosci.* **18** 1–10
[55] Yin J, Han Q, Zhang J, Liu Y, Gan X, Xie K, Xie L and Deng Y 2020 MXene-based hydrogels endow polyetheretherketone with effective osteogenicity and

combined treatment of osteosarcoma and bacterial infection *ACS Appl. Mater. Interfaces* **12** 45891–903
[56] Yang C *et al* 2019 Sodium butyrate-modified sulfonated polyetheretherketone modulates macrophage behavior and shows enhanced antibacterial and osteogenic functions during implant-associated infections *J. Mater. Chem.* B **7** 5541–53
[57] Zhang J, Gao X, Ma D, He S, Du B, Yang W, Xie K, Xie L and Deng Y 2021 Copper ferrite heterojunction coatings empower polyetheretherketone implant with multi-modal bactericidal functions and boosted osteogenicity through synergistic photo/Fenton-therapy *Chem. Eng. J.* **422** 130094
[58] Yuan X, Ouyang L, Luo Y, Sun Z, Yang C, Wang J, Liu X and Zhang X 2019 Multifunctional sulfonated polyetheretherketone coating with beta-defensin-14 for yielding durable and broad-spectrum antibacterial activity and osseointegration *Acta Biomater.* **86** 323–37
[59] Guo C, Lu R, Wang X and Chen S 2021 Antibacterial activity, bio-compatibility and osteogenic differentiation of graphene oxide coating on 3D-network poly-ether-ether-ketone for orthopaedic implants *J. Mater. Sci., Mater. Med.* **32** 135
[60] Liu C, Bai J, Wang Y, Chen L, Wang D, Ni S and Liu H 2021 The effects of three cold plasma treatments on the osteogenic activity and antibacterial property of PEEK *Dent. Mater.* **37** 81–93
[61] Sang S, Wang S, Yang C, Geng Z and Zhang X 2022 Sponge-inspired sulfonated polyetheretherketone loaded with polydopamine-protected osthole nanoparticles and berberine enhances osteogenic activity and prevents implant-related infections *Chem. Eng. J.* **437** 135255
[62] Liu W, Li J, Cheng M, Wang Q, Qian Y, Yeung K W K, Chu P K and Zhang X 2019 A surface-engineered polyetheretherketone biomaterial implant with direct and immunoregulatory antibacterial activity against methicillin-resistant Staphylococcus aureus *Biomaterials* **208** 8–20
[63] Wu T, Zhang X, Chen K, Chen Q, Yu Z, Feng C, Qi J and Zhang D 2022 The antibacterial and wear-resistant nano-ZnO/PEEK composites were constructed by a simple two-step method *J. Mech. Behav. Biomed. Mater.* **126** 104986
[64] Jiang J, You D, Wang Q and Gao G 2022 Novel fabrication and biological characterizations of AgNPs-decorated PEEK with gelatin functional nanocomposite to improve superior biomedical applications *J. Biomater. Sci. Polym. Ed.* **33** 590–604
[65] Wang L, He H, Yang X, Zhang Y, Xiong S, Wang C, Yang X, Chen B and Wang Q 2021 Bimetallic ions regulated PEEK of bone implantation for antibacterial and osteogenic activities *Mater. Today Adv.* **12** 100162
[66] Li M *et al* 2017 Construction of functional coatings with durable and broad-spectrum antibacterial potential based on mussel-inspired dendritic polyglycerol and *in situ*-formed copper nanoparticles *ACS Appl. Mater. Interfaces* **9** 35411–8
[67] Seuss S, Heinloth M and Boccaccini A R 2016 Development of bioactive composite coatings based on combination of PEEK, bioactive glass and Ag nanoparticles with antibacterial properties *Surf. Coat. Technol.* **301** 100–5
[68] Yang S, Yu W, Zhang J, Han X, Wang J, Sun D, Shi R, Zhou Y, Zhang H and Zhao J 2022 The antibacterial property of zinc oxide/graphene oxide modified porous polyetheretherketone against S. sanguinis, F. nucleatum and P. gingivalis *Biomed. Mater.* **17** 025013
[69] Sies H and Jones D P 2020 Reactive oxygen species (ROS) as pleiotropic physiological signalling agents *Nat. Rev. Mol. Cell Biol.* **21** 363–83
[70] Azzam E I, Jay-Gerin J P and Pain D 2012 Ionizing radiation-induced metabolic oxidative stress and prolonged cell injury *Cancer Lett.* **327** 48–60
[71] Maier P, Hartmann L, Wenz F and Herskind C 2016 Cellular pathways in response to ionizing radiation and their targetability for tumor radiosensitization *Int. J. Mol. Sci.* **17** 102
[72] Dwyer D J, Kohanski M A and Collins J J 2009 Role of reactive oxygen species in antibiotic action and resistance *Curr. Opin. Microbiol.* **12** 482–9
[73] Kessler A, Hedberg J, Blomberg E and Odnevall I 2022 Reactive oxygen species formed by metal and metal oxide nanoparticles in physiological media—a review of reactions of importance to nanotoxicity and proposal for categorization *Nanomaterials* **12** 1922
[74] Xiao T, Fan L, Liu R, Huang X, Wang S, Xiao L, Pang Y, Li D, Liu J and Min Y 2021 Fabrication of dexamethasone-loaded dual-metal–organic frameworks on polyetheretherketone implants with bacteriostasis and angiogenesis properties for promoting bone regeneration *ACS Appl. Mater. Interfaces* **13** 50836–50
[75] Xue Z, Wang Z, Sun A, Huang J, Wu W, Chen M, Hao X, Huang Z, Lin X and Weng S 2020 Rapid construction of polyetheretherketone (PEEK) biological implants incorporated with brushite ($CaHPO_4{\cdot}2H_2O$) and antibiotics for anti-infection and enhanced osseointegration *Mater. Sci. Eng.* C **111** 110782
[76] Lau N C, Lai Y C, Chen D W and Cheng K W 2022 Antibacterial activity studies of 3D-printing polyetheretherketone substrates with surface growth of 2D $TiO_2$/ZnO rodlike arrays *ACS Omega* **7** 9559–72
[77] Gao A, Hang R, Huang X, Zhao L, Zhang X, Wang L, Tang B, Ma S and Chu P K 2014 The effects of titania nanotubes with embedded silver oxide nanoparticles on bacteria and osteoblasts *Biomaterials* **35** 4223–35
[78] Dorovskikh S I *et al* 2022 Biological studies of new implant materials based on carbon and polymer carriers with film heterostructures containing noble metals *Biomedicines* **10** 2230
[79] Shuai C, Shuai C, Feng P, Gao C, Peng S and Yang Y 2018 Antibacterial capability, physicochemical properties, and biocompatibility of n$TiO_2$ incorporated polymeric scaffolds *Polymers* **10** 328
[80] Chen T, Chen Q, Fu H, Wang D, Gao Y, Zhang M and Liu H 2021 Construction and performance evaluation of a sustained release implant material polyetheretherketone with antibacterial properties *Mater. Sci. Eng.* C **126** 112109
[81] Qi D, Wang N, Cheng Y, Zhao Y, Meng L, Yue X, She P and Gao H 2022 Application of porous polyetheretherketone scaffold/vancomycin-loaded thermosensitive hydrogel composites for antibacterial therapy in bone repair *Macromol. Biosci.* **22** 1–10
[82] Cai G *et al* 2020 Hierarchically porous surface of PEEK/nMCS composite created by femtosecond laser and incorporation of resveratrol exhibiting antibacterial performances and osteogenic activity *in vitro Composites* B **186** 107802
[83] Abdulkareem M H, Abdalsalam A H and Bohan A J 2019 Influence of chitosan on the antibacterial activity of composite coating (PEEK /HAp) fabricated by electrophoretic deposition *Prog. Org. Coat.* **130** 251–9
[84] Ding R, Chen T, Xu Q, Wei R, Feng B, Weng J, Duan K, Wang J, Zhang K and Zhang X 2020 Mixed modification of the surface microstructure and chemical state of polyetheretherketone to improve its antimicrobial activity, hydrophilicity, cell adhesion, and bone integration *ACS Biomater. Sci. Eng.* **6** 842–51
[85] Meng X, Zhang J, Chen J, Nie B, Yue B, Zhang W, Lyu Z, Long T and Wang Y 2020 KR-12 coating of polyetheretherketone (PEEK) surface: via polydopamine improves osteointegration and antibacterial activity *in vivo J. Mater. Chem.* B **8** 10190–204
[86] Jacob B, Park I S, Bang J K and Shin S Y 2013 Short KR-12 analogs designed from human cathelicidin LL-37 possessing both antimicrobial and antiendotoxic activities without mammalian cell toxicity *J. Pept. Sci.* **19** 700–7

[87] Li Y, Xiang Q, Zhang Q, Huang Y and Su Z 2012 Overview on the recent study of antimicrobial peptides: origins, functions, relative mechanisms and application *Peptides* **37** 207–15
[88] Hu C-C, Kumar S R, Vi T T T, Huang Y-T, Chen D W and Lue S J 2021 Facilitating GL13K peptide grafting on polyetheretherketone via 1-ethyl-3-(3-dimethylaminopropyl)carbodiimide: surface properties and antibacterial activity *Int. J. Mol. Sci.* **23** 359
[89] Hu K, Yang Z, Zhao Y, Wang Y, Luo J, Tuo B and Zhang H 2022 Bioinspired surface functionalization of poly(ether ether ketone) for enhancing osteogenesis and bacterial resistance *Langmuir* **38** 5924–33
[90] Montero J F D, Barbosa L C A, Pereira U A, Barra G M, Fredel M C, Benfatti C A M, Magini R S, Pimenta A L and Souza J C M 2016 Chemical, microscopic, and microbiological analysis of a functionalized poly-ether-ether-ketone-embedding antibiofilm compounds *J. Biomed. Mater. Res.* A **104** 3015–20
[91] Wang L, He S, Wu X, Liang S, Mu Z, Wei J, Deng F, Deng Y and Wei S 2014 Polyetheretherketone/nano-fluorohydroxyapatite composite with antimicrobial activity and osseointegration properties *Biomaterials* **35** 6758–75
[92] Sun X, Yu C, Zhang L, Cao J, Kaleli E H and Xie G 2022 Tribological and antibacterial properties of polyetheretherketone composites with black phosphorus nanosheets *Polymers* **14** 1242
[93] Li J, Qian S, Ning C and Liu X 2016 RBMSC and bacterial responses to isoelastic carbon fiber-reinforced poly(ether-ether-ketone) modified by zirconium implantation *J. Mater. Chem.* B **4** 96–104
[94] Qin W, Ma J, Liang Q, Li J and Tang B 2021 Tribological, cytotoxicity and antibacterial properties of graphene oxide/carbon fibers/polyetheretherketone composite coatings on Ti–6Al–4V alloy as orthopedic/dental implants *J. Mech. Behav. Biomed. Mater.* **122** 104659
[95] Braem A, Van Mellaert L, Mattheys T, Hofmans D, De Waelheyns E, Geris L, Anné J, Schrooten J and Vleugels J 2014 Staphylococcal biofilm growth on smooth and porous titanium coatings for biomedical applications *J. Biomed. Mater. Res.* A **102** 215–24
[96] Absolom D R, Lamberti F V, Policova Z, Zingg W, van Oss C J and Neumann A W 1983 Surface thermodynamics of bacterial adhesion *Appl. Environ. Microbiol.* **46** 90–97
[97] Gao C, Wang Y, Han F, Yuan Z, Li Q, Shi C, Cao W, Zhou P, Xing X and Li B 2017 Antibacterial activity and osseointegration of silver-coated poly(ether ether ketone) prepared using the polydopamine-assisted deposition technique *J. Mater. Chem.* B **5** 9326–36
[98] Yan J, Xia D, Zhou W, Li Y, Xiong P, Li Q, Wang P, Li M, Zheng Y and Cheng Y 2020 pH-responsive silk fibroin-based CuO/Ag micro/nano coating endows polyetheretherketone with synergistic antibacterial ability, osteogenesis, and angiogenesis *Acta Biomater.* **115** 220–34
[99] Ouyang L, Zhao Y, Jin G, Lu T, Li J, Qiao Y, Ning C, Zhang X, Chu P K and Liu X 2016 Influence of sulfur content on bone formation and antibacterial ability of sulfonated PEEK *Biomaterials* **83** 115–26
[100] Luo S, Wang P, Ma M, Pan Z, Lu L, Yin F and Cai J 2022 Genistein loaded into microporous surface of nano tantalum/PEEK composite with antibacterial effect regulating cellular response *in vitro*, and promoting osseointegration *in vivo J. Mech. Behav. Biomed. Mater.* **125** 104972
[101] Xu A, Zhou L, Deng Y, Chen X, Xiong X, Deng F and Wei S 2016 A carboxymethyl chitosan and peptide-decorated polyetheretherketone ternary biocomposite with enhanced antibacterial activity and osseointegration as orthopedic/dental implants *J. Mater. Chem.* B **4** 1878–90
[102] Zhang J, Wei W, Yang L, Pan Y, Wang X, Wang T, Tang S, Yao Y, Hong H and Wei J 2018 Stimulation of cell responses and bone ingrowth into macro-microporous implants of nano-bioglass/polyetheretherketone composite and enhanced antibacterial activity by release of hinokitiol *Colloids Surf.* B **164** 347–57
[103] He M, Hou Y, Jiang Y, Li Y, Zou Q, Chen C, Zhang L and Yang W 2019 Quaternization on polyetheretherketone and its antimicrobial activity *Mater. Lett.* **235** 242–5
[104] Buwalda S, Rotman S, Eglin D, Moriarty F, Bethry A, Garric X, Guillaume O and Nottelet B 2020 Synergistic anti-fouling and bactericidal poly(ether ether ketone) surfaces via a one-step photomodification *Mater. Sci. Eng.* C **111** 110811
[105] Zhang Y, Wu H, Yuan B, Zhu X, Zhang K and Zhang X 2021 Enhanced osteogenic activity and antibacterial performancein vitroof polyetheretherketone by plasma-induced graft polymerization of acrylic acid and incorporation of zinc ions *J. Mater. Chem.* B **9** 7506–15
[106] Ouyang L, Deng Y, Yang L, Shi X, Dong T, Tai Y, Yang W and Chen Z 2018 Graphene-oxide-decorated microporous polyetheretherketone with superior antibacterial capability and *in vitro* osteogenesis for orthopedic implant *Macromol. Biosci.* **18** 1–13
[107] Chen M, Ouyang L, Lu T, Wang H, Meng F, Yang Y, Ning C, Ma J and Liu X 2017 Enhanced bioactivity and bacteriostasis of surface fluorinated polyetheretherketone *ACS Appl. Mater. Interfaces* **9** 16824–33
[108] Yang X, Chai H, Guo L, Jiang Y, Xu L, Huang W, Shen Y, Yu L, Liu Y and Liu J 2021 *In situ* preparation of porous metal-organic frameworks ZIF-8@Ag on poly-ether-ether-ketone with synergistic antibacterial activity *Colloids Surf.* B **205** 111920
[109] Wang S, Duan C, Yang W, Gao X, Shi J, Kang J, Deng Y, Shi X L and Chen Z G 2020 Two-dimensional nanocoating-enabled orthopedic implants for bimodal therapeutic applications *Nanoscale* **12** 11936–46
[110] Kakinuma H, Ishii K, Ishihama H, Honda M, Toyama Y, Matsumoto M and Aizawa M 2015 Antibacterial polyetheretherketone implants immobilized with silver ions based on chelate-bonding ability of inositol phosphate: processing, material characterization, cytotoxicity, and antibacterial properties *J. Biomed. Mater. Res.* A **103** 57–64
[111] Zhang W, Liu J, Wang H, Xu Y, Wang P, Ji J and Chu P K 2015 Enhanced cytocompatibility of silver-containing biointerface by constructing nitrogen functionalities *Appl. Surf. Sci.* **349** 327–32
[112] Zhang W, Wang H, Oyane A, Tsurushima H and Chu P K 2011 Osteoblast differentiation and disinfection induced by nitrogen plasma-treated surfaces *Biomed. Mater. Eng.* **21** 75–82
[113] Niu Y, Guo L, Hu F, Ren L, Zhou Q, Ru J and Wei J 2020 Macro-microporous surface with sulfonic acid groups and micro-nano structures of peek/ nano magnesium silicate composite exhibiting antibacterial activity and inducing cell responses *Int. J. Nanomed.* **15** 2403–17
[114] Raslan A, Saenz Del Burgo L, Ciriza J and Luis Pedraz J 2020 Graphene oxide and reduced graphene oxide-based scaffolds in regenerative medicine *Int. J. Pharm.* **580** 119226
[115] Mei S, Wang F, Hu X, Yang K, Xie D, Yang L, Wu Z and Wei J 2021 Construction of a hierarchical micro & nanoporous surface for loading genistein on the composite of polyetheretherketone/tantalum pentoxide possessing antibacterial activity and accelerated osteointegration *Biomater. Sci.* **9** 167–85
[116] Wang Y, Jin Y, Chen Y, Han T, Chen Y and Wang C 2022 A preliminary study on surface bioactivation of polyaryletherketone by UV-grafting with PolyNaSS: influence on osteogenic and antibacterial activities *J. Biomater. Sci. Polym. Ed.* **33** 1845–65
[117] Deng Y, Yang L, Huang X, Chen J, Shi X, Yang W, Hong M, Wang Y, Dargusch M S and Chen Z G 2018 Dual Ag/ZnO-decorated micro-/nanoporous sulfonated polyetheretherketone with superior antibacterial capability and biocompatibility via layer-by-layer self-assembly strategy *Macromol. Biosci.* **18** 1–12

[118] Sandra W R and David R 1991 Polymeric film coated in-line with polyethyleneimine *European Patent* US5156904A pp 1–9
[119] Hu Q, Wang Y, Liu S, Liu Q and Zhang H 2022 3D printed polyetheretherketone bone tissue substitute modified via amoxicillin-laden hydroxyapatite nanocoating *J. Mater. Sci.* **57** 18601–14
[120] Wang F, Wang M, He Q, Wang X, Sun P, Ji Y, Niu Y, Li F and Wei J 2023 Black tantalic oxide submicro-particles coating on PEEK fibers woven into fabrics as artificial ligaments with photothermal antibacterial effect and osteogenic activity for promoting ligament-bone healing *J. Mater. Sci. Technol.* **133** 195–208
[121] Yu X, Ibrahim M, Liu Z, Yang H, Tan L and Yang K 2018 Biofunctional Mg coating on PEEK for improving bioactivity *Bioact. Mater.* **3** 139–43
[122] Hsieh J H, Li C, Lin Y C, Chiu C H, Hu C C and Chang Y H 2015 Antibacteria and anti-wear TaN-(Ag,Cu) nanocomposite thin films deposited on polyether ether ketone *Thin Solid Films* **584** 277–82
[123] He X, Deng Y, Yu Y, Lyu H and Liao L 2019 Drug-loaded/grafted peptide-modified porous PEEK to promote bone tissue repair and eliminate bacteria *Colloids Surf.* B **181** 767–77
[124] Cruz-Pacheco A, Muñoz-Castiblanco D, Gómez Cuaspud J, Paredes-Madrid L, Parra Vargas C, Martínez Zambrano J and Palacio Gómez C 2019 Coating of polyetheretherketone films with silver nanoparticles by a simple chemical reduction method and their antibacterial activity *Coatings* **9** 91
[125] Ur Rehman M A, Ferraris S, Goldmann W H, Perero S, Bastan F E, Nawaz Q, Confiengo G G D, Ferraris M and Boccaccini A R 2017 Antibacterial and bioactive coatings based on radio frequency co-sputtering of silver nanocluster-silica coatings on PEEK/bioactive glass layers obtained by electrophoretic deposition *ACS Appl. Mater. Interfaces* **9** 32489–97
[126] Lyu Z, Zhao Y, Huo S, Wang F, Meng X, Yuan Z, Long T and Wang Y 2022 Mussel-inspired dopamine-CuII coated polyetheretherketone surface with direct and immunomodulatory effect to facilitate osteogenesis, angiogenesis, and antibacterial ability *Mater. Des.* **222** 111069
[127] Sun A, Lin X, Xue Z, Huang J, Bai X, Huang L, Lin X, Weng S and Chen M 2021 Facile surface functional polyetheretherketone with antibacterial and immunoregulatory activities for enhanced regeneration toward bacterium-infected bone destruction *Drug. Deliv.* **28** 1649–63
[128] Xu Z *et al* 2019 A hierarchical nanostructural coating of amorphous silicon nitride on polyetheretherketone with antibacterial activity and promoting responses of rBMSCs for orthopedic applications *J. Mater. Chem.* B **7** 6035–47
[129] He M, Zhu C, Xu H, Sun D, Chen C, Feng G, Liu L, Li Y and Zhang L 2020 Conducting polyetheretherketone nanocomposites with an electrophoretically deposited bioactive coating for bone tissue regeneration and multimodal therapeutic applications *ACS Appl. Mater. Interfaces* **12** 56924–34
[130] Zhang Q, Sando D and Nagarajan V 2016 Chemical route derived bismuth ferrite thin films and nanomaterials *J. Mater. Chem.* C **4** 4092–124
[131] Shi F 2018 Introductory chapter: basic theory of magnetron sputtering *Magnetron Sputtering* vol 11 (IntechOpen) p 13
[132] Rahim S A, Joseph M A, Sampath Kumar T S and T H 2022 Recent progress in surface modification of Mg alloys for biodegradable orthopedic applications *Front. Mater.* **9** 1–21
[133] Xian P, Chen Y, Gao S, Qian J, Zhang W, Uddutula A, Huang N and Wan G 2020 Polydopamine (PDA) mediated nanogranular-structured titanium dioxide ($TiO_2$) coating on polyetheretherketone (PEEK) for oral and maxillofacial implants application *Surf. Coat. Technol.* **401** 126282
[134] Zou F, Lv F, Ma X, Xia X, Cai L, Mei S, Wei J, Niu Y and Jiang J 2020 Dual drugs release from nanoporously bioactive coating on polyetheretherketone for enhancement of antibacterial activity, rBMSCs responses and osseointegration *Mater. Des.* **188** 108433
[135] Chen Y, Yang Q, Ma D, Peng L, Mao Y, Zhou X, Deng Y and Yang W 2022 Metal-organic frameworks/polydopamine coating endows polyetheretherketone with disinfection and osteogenicity *Int. J. Polym. Mater. Polym. Biomater.* **71** 783–94
[136] Garcia D, Gilmore A, Berns E, Spake C, Dockery D M, Vishwanath N, Glasser J, Antoci V, Daniels A and Born C T 2021 Silver carboxylate and titanium dioxide-polydimethylsiloxane coating decreases adherence of multi-drug resistant Serratia marcescens on spinal implant materials *Spine Deform.* **9** 1493–500
[137] Yan J, Xia D, Xiong P, Li Y, Zhou W, Li Q, Wang P, Zheng Y and Cheng Y 2021 Polyetheretherketone with citrate potentiated influx of copper boosts osteogenesis, angiogenesis, and bacteria-triggered antibacterial abilities *J. Mater. Sci. Technol.* **71** 31–43
[138] Deng Y, Shi X, Chen Y, Yang W, Ma Y, Shi X L, Song P, Dargusch M S and Chen Z G 2020 Bacteria-triggered pH-responsive osteopotentiating coating on 3D-printed polyetheretherketone scaffolds for infective bone defect repair *Ind. Eng. Chem. Res.* **59** 12123–35
[139] Sikder P, Grice C R, Lin B, Goel V K and Bhaduri S B 2018 Single-phase, antibacterial trimagnesium phosphate hydrate coatings on polyetheretherketone (PEEK) implants by rapid microwave irradiation technique *ACS Biomater. Sci. Eng.* **4** 2767–83
[140] Simchi A, Tamjid E, Pishbin F and Boccaccini A R 2011 Recent progress in inorganic and composite coatings with bactericidal capability for orthopaedic applications *Nanomedicine* **7** 22–39
[141] Abouaitah K *et al* 2021 Drug-releasing antibacterial coating made from nano-hydroxyapatite using the sonocoating method *Nanomaterials* **11** 1690
[142] Sang S, Yang C, Chai H, Yuan X, Liu W and Zhang X 2021 The sulfonated polyetheretherketone with 3D structure modified by two bio-inspired methods shows osteogenic and antibacterial functions *Chem. Eng. J.* **420** 130059
[143] Borgolte M, Riester O, Quint I, Blendinger F, Bucher V, Laufer S, Csuk R, Scotti L and Deigner H P 2022 Synthesis of a biocompatible benzophenone-substituted chitosan hydrogel as novel coating for PEEK with extraordinary strong antibacterial and anti-biofilm properties *Mater. Today Chem.* **26** 101176
[144] Wu P, Hu S, Liang Q, Guo W, Xia Y, Shuai C and Li Y 2020 A polymer scaffold with drug-sustained release and antibacterial activity *Int. J. Polym. Mater. Polym. Biomater.* **69** 398–405
[145] Wu P, Liang Q, Feng P, Li C, Yang C, Liang H, Tang H and Shuai C 2017 A novel brucine gel transdermal delivery system designed for anti-inflammatory and analgesic activities *Int. J. Mol. Sci.* **18** 1–12
[146] Yin W, Zhou C, Ju X, Deng Y, Zhang L and Xie R 2022 Dual-functional polyetheretherketone surface with programmed sequential drug release coating *Colloids Surf.* B **219** 112806
[147] Lau N C, Tsai M H, Chen D W, Chen C H and Cheng K W 2020 Preparation and characterization for antibacterial activities of 3D printing polyetheretherketone disks coated with various ratios of ampicillin and vancomycin salts *Appl. Sci.* **10** 1–14
[148] Li B, Shu R, Dai W, Yang F, Xu H, Shi X, Li Y, Bai D, Yang W and Deng Y 2022 Bioheterojunction-engineered polyetheretherketone implants with diabetic infectious micromilieu twin-engine powered disinfection for boosted osteogenicity *Small* **18** 1–17
[149] Hu G, Zhu Y, Xu F, Ye J, Guan J, Jiang Y, Di M, Li Z, Guan H and Yao X 2022 Comparison of surface properties,

cell behaviors, bone regeneration and osseointegration between nano tantalum/PEEK composite and nano silicon nitride/PEEK composite *J. Biomater. Sci. Polym. Ed.* **33** 35–56

[150] Feng C, Cen J, Wu T, Hou T, Chen K, Li X and Zhang D 2022 Preparation and properties of the poly(ether ether ketone) (PEEK)/nano-zinc oxide (ZnO)-short carbon fiber (SCF) artificial joint composites *ACS Appl. Polym. Mater.* **4** 8869–77

[151] Yang A, Guo W, Han T, Zhao C, Zhou H and Cai J 2021 Feedback control of injection rate of the injection molding machine based on PID improved by unsaturated integral *Shock Vib.* **2021** 1–9

[152] Rider P, Kačarević Ž, Alkildani S, Retnasingh S, Schnettler R and Barbeck M 2018 Additive manufacturing for guided bone regeneration: a perspective for alveolar ridge augmentation *Int. J. Mol. Sci.* **19** 3308

[153] Guo J, Pfeiffenberger N, Beese A, Rhoades A, Gao L, Baker A, Wang K, Bolvari A and Randall C A 2018 Cold sintering $Na_2Mo_2O_7$ ceramic with poly(ether imide) (PEI) polymer to realize high-performance composites and integrated multilayer circuits *ACS Appl. Nano Mater.* **1** 3837–44

[154] Díez-Pascual A M, Xu C and Luque R 2014 Development and characterization of novel poly(ether ether ketone)/ZnO bionanocomposites *J. Mater. Chem.* B **2** 3065–78

[155] Ru X, Chu M, Jiang J, Yin T, Li J and Gao S 2023 Polyetheretherketone/Nano-Ag-$TiO_2$ composite with mechanical properties and antibacterial activity *J. Appl. Polym. Sci.* **140** 1–11

[156] Peter A, Lutey A H A, Faas S, Romoli L, Onuseit V and Graf T 2020 Direct laser interference patterning of stainless steel by ultrashort pulses for antibacterial surfaces *Opt. Laser Technol.* **123** 105954

[157] Adlhart C, Verran J, Azevedo N F, Olmez H, Keinänen-Toivola M M, Gouveia I, Melo L F and Crijns F 2018 Surface modifications for antimicrobial effects in the healthcare setting: a critical overview *J. Hosp. Infection* **99** 239–49

[158] Lutey A H A, Gemini L, Romoli L, Lazzini G, Fuso F, Faucon M and Kling R 2018 Towards laser-textured antibacterial surfaces *Sci. Rep.* **8** 1–10

[159] Lazzini G, Romoli L, Lutey A H A and Fuso F 2019 Modelling the interaction between bacterial cells and laser-textured surfaces *Surf. Coat. Technol.* **375** 8–14

[160] Graham M V and Cady N C 2014 Nano and microscale topographies for the prevention of bacterial surface fouling *Coatings* **4** 37–59

[161] Lu T, Li J, Qian S, Cao H, Ning C and Liu X 2016 Enhanced osteogenic and selective antibacterial activities on micro-/nano-structured carbon fiber reinforced polyetheretherketone *J. Mater. Chem.* B **4** 2944–53

[162] Wang X, Lu T, Wen J, Xu L, Zeng D, Wu Q, Cao L, Lin S, Liu X and Jiang X 2016 Selective responses of human gingival fibroblasts and bacteria on carbon fiber reinforced polyetheretherketone with multilevel nanostructured $TiO_2$ *Biomaterials* **83** 207–18

[163] Akhtar J, Abrha M G, Teklehaimanot K and Gebrekirstos G 2022 Cold plasma technology: fundamentals and effect on quality of meat and its products *Food Agric. Immunol.* **33** 451–78

[164] Sant'Ana P L, Bortoleto J R, da Cruz N C, Rangel E C, Durrant S F, Botti L M and Dos Anjos C A 2020 Surface properties of low-density polyethylene treated by plasma immersion ion implantation for food packaging *Rev. Bras. Apl. Vácuo* **39** 14–23

[165] Zhao Z, Cao Y, Cai Y, Yang J, He X, Nordlander P and Cremer P S 2017 Oblique colloidal lithography for the fabrication of nonconcentric features *ACS Nano* **11** 6594–604

[166] Lu T, Liu X, Qian S, Cao H, Qiao Y, Mei Y, Chu P K and Ding C 2014 Multilevel surface engineering of nanostructured $TiO_2$ on carbon-fiber-reinforced polyetheretherketone *Biomaterials* **35** 5731–40

[167] Gan K, Liu H, Jiang L, Liu X, Song X, Niu D, Chen T and Liu C 2016 Bioactivity and antibacterial effect of nitrogen plasma immersion ion implantation on polyetheretherketone *Dent. Mater.* **32** e263–74

[168] Mo S, Mehrjou B, Tang K, Wang H, Huo K, Qasim A M, Wang G and Chu P K 2020 Dimensional-dependent antibacterial behavior on bioactive micro/nano polyetheretherketone (PEEK) arrays *Chem. Eng. J.* **392** 123736

[169] Siegel J, Vyhnálková B, Savenkova T, Pryjmaková J, Slepička P, Šlouf M and Hubáček T 2023 Surface engineering of AgNPs-decorated polyetheretherketone *Int. J. Mol. Sci.* **24** 1432

[170] Ucar Y, Ceylan Z, Durmus M, Tomar O and Cetinkaya T 2021 Application of cold plasma technology in the food industry and its combination with other emerging technologies *Trends Food Sci. Technol.* **114** 355–71

[171] Mo S *et al* 2022 Tuning the arrangement of lamellar nanostructures: achieving the dual function of physically killing bacteria and promoting osteogenesis *Mater. Horiz.* **10** 881–8

[172] Mantese J V, Brown I G, Cheung N W and Collins G A 1996 Plasma-immersion ion implantation *MRS Bull.* **21** 52–56

[173] Thomae R W 1998 Plasma-immersion ion implantation *Nucl. Instrum. Methods Phys. Res.* B **139** 37–42

[174] Lu M, Xuan S and Wang Z 2019 Oral microbiota: a new view of body health *Food Sci. Hum. Wellness* **8** 8–15

[175] Montoya C, Roldan L, Yu M, Valliani S, Ta C, Yang M and Orrego S 2023 Smart dental materials for antimicrobial applications *Bioact. Mater.* **24** 1–19

[176] Puri S, Orrego S, Montoya C, Kurylec J, Baraniya D and Tripathi A 2021 Antifungal effect of piezoelectric charges on pmma dentures *ACS Biomater. Sci. Eng.* **7** 4838–46